

T.C.

AYDIN ADNAN MENDERES UNIVERSITY

GRADUATE SCHOOL OF NATURAL AND APPLIED SCIENCES

MASTER'S PROGRAMME IN MECHANICAL ENGINEERING



EAGLE EYE

Kadir KARACA

MASTER'S THESIS

SUPERVISOR

Prof. Dr. Ismail BOGREKCI

AYDIN-2022

APPROVAL AND ACCEPTANCE

The thesis titled “EAGLE EYE”, prepared by Kadir KARACA a student of Department Of Mechanical Engineering at T.C. Aydin Adnan Menderes University, Graduate School Of Natural And Applied Science, was accepted as a Master's Thesis by the jury below.

Date of Thesis Defense: 03/08/2022

	Title, Name Surname	Institution	Signature
Member:	Prof. Dr. Ismail BOGREKCI	Aydin Adnan Menderes University	
Member:	Prof. Dr. Pinar DEMIRCIOGLU	Aydin Adnan Menderes University	
Member:	Assoc. Prof. Dr. Arzum ISITAN	Pamukkale University	

APPROVAL:

This thesis was approved by the jury above in accordance with the relevant articles of the Aydin Adnan Menderes University Graduate Education and Examination Regulations and was approved on the by from the Board of Directors of the Graduate School of Science in the numbered decision.

Prof. Dr. Gönül AYDIN
Institute Director

ACKNOWLEDGEMENTS

In the realization of this study, my esteemed and advisor Prof. Dr. İsmail BOGREKCI, who shared his valuable knowledge with me, spared his precious time for me whenever I consulted him, took care of me with patience and great interest, whom I could go to without hesitation whenever I had a problem, and who never spared me his smiling face and sincerity. I thank you and express my gratitude.

I would also like to thank my beloved family, who supported me and showed great patience during this difficult work.

Kadir KARACA

TABLE OF CONTENTS

APPROVAL AND ACCEPTANCE	i
ACKNOWLEDGEMENTS.....	ii
TABLE OF CONTENTS	iii
A LIST OF SYMBOLS AND ABBREVIATIONS	vi
LIST OF FIGURES	viii
LIST OF TABLES.....	xi
ÖZET	xi
ABSTRACT	xiii
1. INTRODUCTION	1
1.1. World Aviation History	1
1.2. Aviation History in Turkey.....	2
2. LITERATURE REVIEW	3
2.1. General Information About Uavs	3
2.1.1. Tricopter UAV.....	3
2.1.2. VTOL UAV	4
2.2. Investigation Of Flight Aerodynamics	4
2.2.1. Flight Mechanics	5
2.2.1.1. Forces Acting on Flight.....	5
2.2.1.2. Forces and Moments Affecting Flight.....	6
2.2.1.2.1. Reynolds Number.....	6
2.2.1.2.2. Mach Number	7
2.3. Airfoils Aerodynamics	8
2.3.1. General Features of an Airfoil.....	8
2.3.2. NACA Airfoils	9

2.3.2.1. Four-Digit NACA Airfoils	10
2.3.2.2. Five-Digit NACA Airfoils.....	10
2.3.2.3. The 6-Series NACA Airfoils	10
3. MATERIAL AND METHOD.....	11
3.1. Preliminary Design.....	11
3.2. Wing Design.....	17
3.2.1. Number Of Wing.....	17
3.2.2. Wing Vertical Location	18
3.2.3. Airfoil Section	19
3.2.3.1. The Wing Maximum Thickness To-Chord Ratio.....	20
3.2.3.2. The Angle Of Attack	21
3.2.3.3. Swept Wing	24
3.2.3.4. Dihedral Angle	25
3.2.3.5. Camber Ratio.....	26
3.3. Wing Airfoil Section Selection.....	26
3.3.1. Wing 3D Model Design.....	29
3.4. Fuselage Design.....	31
3.4.1. Fuselage Airfoil Section Selection	31
3.4.2. Fuselage 3D Model Design	34
3.5. Body Assembly.....	35
4. RESULTS.....	36
4.1. Wing Flow Simulation.....	36
4.2. Fuselage Flow Simulation	38
4.3. Body Flow Simulation.....	40
5. DISCUSSION.....	42
6. CONCLUSION AND RECOMMENDATIONS	43

7. APPENDICES	44
REFERENCES	45
SCIENTIFIC ETHICAL STATEMENT.....	47
CURRICULUM VITAE.....	48



A LIST OF SYMBOLS AND ABBREVIATIONS

Avg	: Average
UAV	: Unmanned aerial vehicle
VTOL	: Vertical Take-Off And Landing
NACA	: National Advisory Committee for Aeronautics
L	: Lift Force (N)
W	: Weight (N)
V_{∞}	: Cruising Speed (m/sn)
Max	: Maximum
Min	: Minimum
V_S	: Stall Speed
Re	: Reynolds Number
Ma	: Mach Number
WTO	: Maximum Take-Off Weight
S_{Ref} , S_w	: Wing Reference Area (m^2)
V_{Max}	: Maximum Speed, (m/sn)
STOL	: Short take-off and landing
h_{Max}	: Maximum Cruising Height (m)
AR	: Aspect Ratio
B	: Wingspan (m)
$(t/c)_{root}$: The Wing Maximum Thickness To-Chord Ratio
A	: The Angle Of Attack (degr,rad)
Γ	: Dihedral Angle (degr,rad)
N	: Rotational speed (rpm,rad/s)
Λ	: Sweep Angle (deg,rad)

Γ : Camber Ratio
 Λ : Taper Ratio
cr : Root Chord
ct : Tip Chord



LIST OF FIGURES

Figure 1.1. Heinkel He 178.....	1
Figure 1.2. Nuri DEMİRAĞ.....	2
Figure 2.1. Y Frame Design Tricopter.....	3
Figure 2.2. VTOL UAV.....	4
Figure 2.3. Fundamental Forces Acting On The Aircraft.....	5
Figure 2.4. Forces-On-Airplane.....	6
Figure 2.5. Boundary Layer Thickness On Flat Plate.	7
Figure 2.6. Airfoil geometric parameters	8
Figure 2.7. Five sample airfoil sections.....	9
Figure 2.8. Four-digit, a five-digit, and a 6-series airfoil section : (a) NACA 1408; (b) NACA 23012; and (c) NACA 633-218.....	10
Figure 3.1. Akıncı TİHA	12
Figure 3.2. The Predator USA	13
Figure 3.3. Delta Quad Pro	14
Figure 3.4. Typical values of wing aspect ratio.....	15
Figure 3.5. Three options in number of wings (front view): (a) Monoplane; (b) Biplane; and (c) Tri-Wing.....	18
Figure 3.6. Options in vertical wing positions: (a) High wing; (b) Mid-wing; (c) Low wing; and (d) Parasol wing.....	18
Figure 3.7. Four aircraft with different wing vertical positions: (a) Lockheed Martin C- 130J Hercules (high wing); (b) Boeing 767 (low wing); (c) Pietenpol Air Camper-2 (parasol wing); (d) Hawker Sea Hawk (mid-wing).....	19
Figure 3.8. Typical airfoil section.....	19
Figure 3.9. The Wing Maximum Thickness To-Chord Ratio.	20
Figure 3.10. Five sample airfoil sections.....	21

Figure 3.11. Chord line and angle of attack (a) Aerofoil with concave undersurface. (b) Aerofoil with flat undersurface. (c) Aerofoil with convex undersurface.	22
Figure 3.12. Lift/drag curve.....	23
Figure 3.13. Effect of slot on airflow over an airfoil at large angle of attack	23
Figure 3.14. Five wings with different sweep angles	24
Figure 3.15. (a) Dihedral and (b) anhedral (aircraft front view)	25
Figure 3.16. The effect of dihedral angle on a disturbance in roll (aircraft front view): (a) before gust; (b) after gust.....	25
Figure 3.17. NACA 64210.....	27
Figure 3.18. Aerodynamic coefficient graphs. a) The variations the lift coefficient versus of the drag coefficient. b) The variations of lift coefficient versus the angle of attack. c) The variations of the lift-to-drag ratio versus the angle of attack. d) The variations of drag coefficient versus the angle of attack. e) The Variations of Pitching Moment Coefficient versus Angle of Attack.....	27
Figure 3.19. NACA 64210 airflows	29
Figure 3.20. 3D Model Wing.....	29
Figure 3.21. Wing Dimensions (root chord, tip chord, wingspan).....	30
Figure 3.22. Left, Right Wing (total wingspan)	30
Figure 3.23. NACA 2414.....	31
Figure 3.24. Aerodynamic coefficient graphs. a) The variations the lift coefficient versus of the drag coefficient. b) The variations of lift coefficient versus the angle of attack. c) The variations of the lift-to-drag ratio versus the angle of attack. d) The variations of drag coefficient versus the angle of attack. e) The Variations of Pitching Moment Coefficient versus Angle of Attack.....	32
Figure 3.25. 2D Model Fuselage Airfoil	34
Figure 3.26. 3D Model Fuselage	34
Figure 3.27. Fuselage Dimensions.....	35
Figure 3.28. Body Assembly	35

Figure 3.29. Body Assembly (Front).....	35
Figure 4.1. Wing Dynamic Pressure.....	36
Figure 4.2. Wing Turbulence Length (Perspective)	36
Figure 4.3. Wing Turbulence Length	37
Figure 4.4. Fuselage Dynamic Pressure	38
Figure 4.5. Fuselage Velocity	38
Figure 4.6. Fuselage Turbulence Length (Perspective)	39
Figure 4.7. Fuselage Turbulence Length	39
Figure 4.8. Body Dynamic Pressure	40
Figure 4.9. Body Velocity	41
Figure.7.1. UAV Vertical Take Off Mode	44
Figure 7.2. UAV Flight Mode	44

LIST OF TABLES

Table 3. 1. Assumptions to be used in theoretical calculations	15
Table 3. 2. Formulas used with calculated values	16
Table 3. 3. Determination of the dihedral angle	26
Table 3.4. Table of coefficients for NACA 64210 depending on the changing angle of attack	28
Table 3.5. Table of coefficients for NACA 2414 depending on the changing angle of attack	34
Table 4.1. Wing Results.....	37
Table 4.2. Fuselage Results	40
Table 4.3 Body Results.....	41

ÖZET

KARTAL GÖZ

Karaca K. Aydın Adnan Menderes Üniversitesi, Fen Bilimleri Enstitüsü, Makine Mühendisliği Programı, Yüksek Lisans Tezi, Aydın, 2022.

Amaç: Havacılık geçmişten günümüze sürekli bir gelişim içerisinde. Son yıllarda İnsansız Hava Aracı (İHA) platformlarına olan talep her geçen gün artmakta ve askeri alanda kullanımı stratejik bir teknoloji haline gelmiştir. İHA'ların fiziksel bir kullanıcıya ihtiyaç olmaması ve üretim maliyetlerinin normal bir hava aracına göre daha düşük olması İHA'ları daha cazip hale getirmektedir. İHA'lar kullanım amacına göre sabit kanatlı, döner kanatlı ve hem sabit hemde döner kanatlı (hibrit) olarak üç ana grupta toplamak mümkündür. Bu çalışmamızda dikey iniş kalkış özelliğine sahip bir İHA'nın kavrsamsal tasarımı ve ön mühendislik hesaplamaları yapılmıştır.

Materyal ve Yöntem: Tasarım sürecine başlamadan önce hava araçlarına etki eden fiziksel ve aerodinamik kuvvetler incelenmiştir. Bu incelememin sonucu olarak hesaplamalar yapılmadan önce bazı ön kabuller yapılmıştır. Bu ön kabuller yapıldıktan sonra ön mühendislik hesaplamaları yapılmıştır. Bu işlemlerden sonra gövde ve kanat tasarımları 3 boyutlu tasarım programı kullanılarak İHA'mızın tasarımı yapılmıştır. Tasarım süreci kanat ve ana gövde profilini hiç denenmemiş bir profil tasarlamak yerine bu Ulusal Havacılık Danışma Komitesi (NACA) tarafından önce bilgisayar ortamında analiz edilmiş ve bu analiz verilerini sonra laboratuvar ortamında fiziksel test yapılarak doğrulanmış profillerden birini seçtik.

Bulgular: Tasarım süreci tamamlandıktan sonra akış analiz programları kullanarak gövdenin, kanatların ayrı ayrı aerodinamik analizlerini yaptıktan sonra gövdeyi ve kanatları bilgisayar ortamında montajlayıp tekrardan aerodinamik analizini yaptık.

Sonuç: Analiz sonuçlarımızda elde ettiğimiz değerler ile ön kabul değerleri karşılaştırdık. Yine gövde ve kanat profilleri olarak seçtiğimiz profillerin teknik verileri ile analizde ettiğimiz sonuçları karşılaştırdık. Yapmış olduğumuz karşılaştırma sonucu olarak değerlerimiz bir birlerine çıktığını tespit ettik ve yapmış olduğumuz tasarımı doğrulamış olduk.

Anahtar Kelime: Aerodinamik, Dikey, Drone, Havalanmak, İHA, Kalkış, Kanat, Sabit, Tricoper, Uçak.

ABSTRACT

EAGLE EYE

Karaca K. Adnan Menderes University, Graduate School of Natural and Applied Science, Department of Mechanical Engineering, Master's Thesis, Aydin, 2022.

Objective: Aviation is in a continuous development from past to present. In recent years, the demand for Unmanned Aerial Vehicle (UAV) platforms has been increasing day by day and its use in the military field has become a strategic technology. The fact that UAVs do not need a physical user and their production costs are lower than a normal aircraft makes UAVs more attractive.

It is possible to collect UAVs in three main groups as fixed wing, rotary wing and both fixed and rotary wing (hybrid) according to the purpose of use. In this study, the conceptual design and preliminary engineering calculations of an UAV with vertical take-off feature were made.

Material and Methods: Before starting the design process, the physical and aerodynamic forces affecting the aircraft were examined. Some preliminary assumptions were made before the calculations were made as the presenter of this review. After these preliminary assumptions were made, preliminary engineering calculations were made. Instead of designing an untested profile for the wing and main body profile in the design process, we chose one of the profiles that were first analyzed by the National Aeronautics Advisory Committee (NACA) in a computer environment and then verified by physical testing in the laboratory environment.

Results: After the design process was completed, we made separate aerodynamic analyzes of the fuselage and wings using flow analysis programs, and then combined the fuselage and wings in the computer environment and performed the aerodynamic analysis again.

Conclusion: We compared the values we obtained in our analysis results with the preliminary acceptance values. Again, we compared the technical data of the profiles we chose as the fuselage and wing profiles with the results we analyzed.

Key Word: Aerodynamic, Aircraft, Drone, Fix Wing, Take-Off, Tricopter, Uav, Vertical.

1. INTRODUCTION

1.1. World Aviation History

- The first balloon flight in 1783.
- 1891 Langley first steam-powered aircraft trial.
- 1903 Wright brothers first time in a heavier-than-air aircraft powered by an engine.

This aircraft had two propellers, with the pilot it weighed 335 kg.

- The Heinkel He 178 aircraft, tested by 1939 German pilot Erich Warsitz (1906–1983), is recorded as the first aircraft in history to take off with a jet engine.

- In 1947, the US pilot Chuck Yeager (1923-2020) flew X-1 aircraft faster than the speed of sound and crossed the sound barrier for the first time. The X-1 also carried a rocket engine and recorded a speed of 1,299 kilometers per hour.(Pehlivanoglu,2013)



Figure 1.1. Heinkel He 178.(Anonymous,2022 a)

1.2. Aviation History in Turkey

• In 1911, Staff Lieutenant Colonel Süreyya (İlmen) Bey was tasked with establishing the aviation organization, and the first official aviation organization of the Turkish Army was launched under the name of "Aviation Commission" within the 2nd branch of the Ministry of War, Science Continents Fortified General Inspectorate.

• In 1912, the Air School was opened in Istanbul Yesilkoy.

• In 1913, First Lieutenant Fethi Bey made the first night flight, and in the same year he broke ground by dropping bombs on the Bulgarian lines in the Balkan War.

• In 1925, Eskişehir Air School was re-established and gave its first graduates.

• In 1925, Tayyare ve Motor Türk Anonim Şirketi (TOMTAŞ) was established in Ankara.

• With a law dated 1 July 1932, aviator personnel were accepted as a separate combat class.

• Nuri DEMİRAĞ aircraft factory was established in 1936.



Figure 1.2. Nuri DEMİRAĞ (Pehlivanoglu,2013)

• In 1938, the twin-engine six-seat ND-38 was produced.

• January 31, 1944 Air Force Command was established.

• The 9th Jet Base Command, established in Balıkesir in 1951, became the first jet base of the Turkish Air Force, and the 191, 192 and 193rd squadrons became the first jet squadrons.(Pehlivanoglu,2013)

2. LITERATURE REVIEW

2.1. General Information About Uavs

The most basic feature of unmanned aerial vehicles (UAV) is that it can be controlled from the outside or autonomously, not by a pilot inside as in other aircraft. (Anonymous,2022b)

To look at the historical development process of drones; In the early days, the production purpose of drones was for use in difficult military operations. Thanks to the development and cheapening of the technology used in drones, drones began to be used for civilian purposes as well. To give a few examples of civilian uses, such as product deliveries, agriculture, infrastructure inspections and drone racing etc.(Anonymous,2022b) In addition to these uses, it has also started to be used as human transportation and air ambulance.

2.1.1. Tricopter UAV

Three brushless motors drones with a Y or T frame design are called tricopters It is more efficient because it consumes less energy than drones with four or more engines.(Sahin and Oktay, 2019)

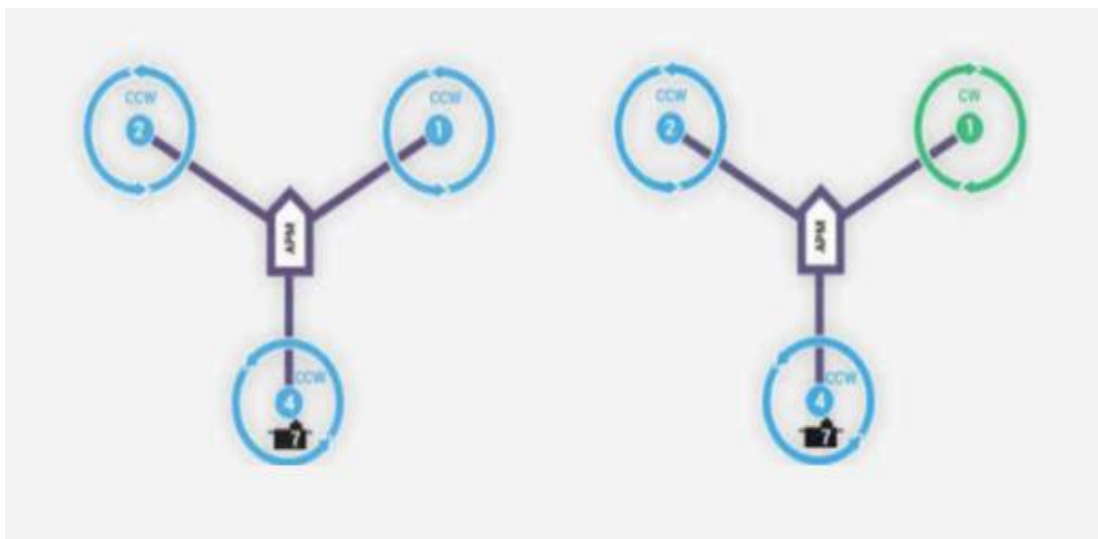


Figure 2.1. Y Frame Design Tricopter (Sahin and Oktay,2019)

2.1.2. VTOL UAV

It is the name given to drones that have both fixed wings and vertical engines (in some models the engine has ± 90 degrees moving). The biggest feature of this type of drones is that they can land and take off vertically.



Figure 2.2. VTOL UAV (Anonymous, 2022 c)

2.2. Investigation Of Flight Aerodynamics

Aerodynamics is a branch of physics that studies the forces acting on a moving mass in air and other gases. It is important in determining the design criteria of vehicles such as aircraft, rockets, high-speed trains and automobiles. It is also a critical factor affecting the structural mechanical calculations of structures such as high-rise buildings and bridges.(Britannica, 2019)

2.2.1. Flight Mechanics

2.2.1.1. Forces Acting on Flight

In aircraft, the fuselage and wings are under the influence of various forces during flight. These forces are thrust, lift, weight and drag forces. An important step in the design process of an aircraft is the calculation of these force values. (U.S. Department of Transportation Federal Aviation Administration, 2016)

The four forces acting on an aircraft in straight-and-level, unaccelerated flight are thrust, drag, lift, and weight. They are defined as follows:

- The thrust force is the force produced by the aircraft engine.
- The drag force is the resistance force of the air that is opposite to the thrust force. The thrust must be greater than the drag force. Otherwise, the aircraft cannot move through the air.
- The lift force is the force that occurs on the fuselage and wings due to the movement of the aircraft and is perpendicular to the flight direction of the aircraft.
- The weight force is called the total weight of the aircraft (the combined load of the aircraft itself, the crew, the fuel, and the cargo or baggage.). The weight pulls the aircraft down due to gravity. The lift force must be greater than this force for the aircraft to rise. (U.S. Department of Transportation Federal Aviation Administration, 2016)

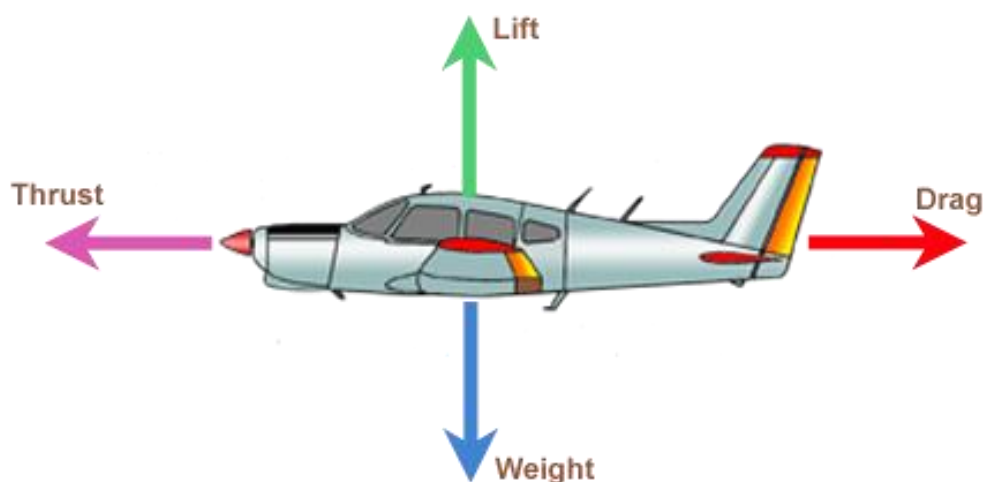


Figure 2.3. Fundamental Forces Acting On The Aircraft.(Anonymous, 2022 d)

2.2.1.2. Forces and Moments Affecting Flight

Lift Force: $L = \frac{1}{2} \rho_{\infty} V_{\infty}^2 S C_L$

Drag Force: $D = \frac{1}{2} \rho_{\infty} V_{\infty}^2 S C_D$

Pitching Moment $M = \frac{1}{2} \rho_{\infty} V_{\infty}^2 S C_M$

The aerodynamic coefficients depend on the angle of attack, geometry (profile geometry, wing geometry, aircraft configuration, wet area, etc.), Reynolds number, and Mach number. The coefficients in this formula will be discussed in more detail in the next sections.

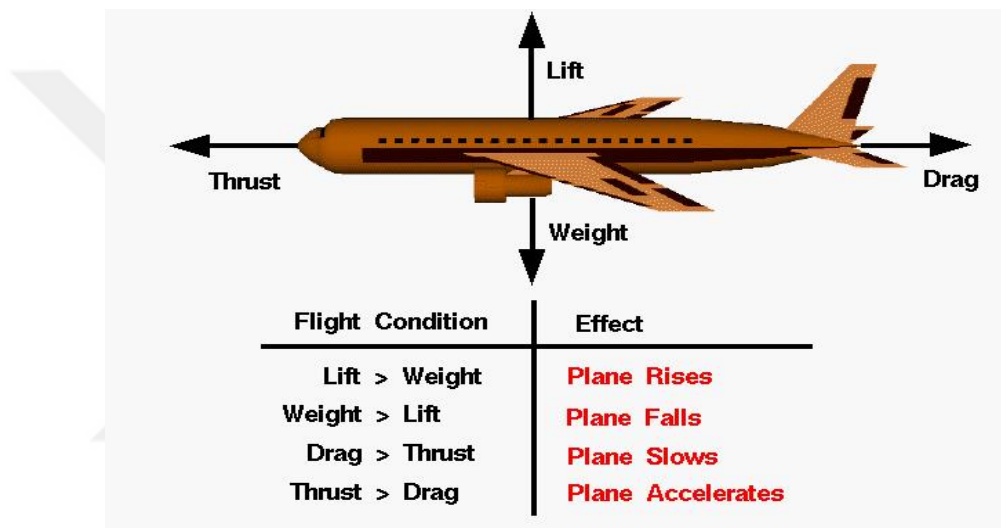


Figure 2.4. Forces-On-Airplane.(Anonymous, 2022 e)

2.2.1.2.1. Reynolds Number

The Reynolds number is the ratio of inertial forces to viscous forces within a fluid which is subjected to relative internal movement due to different fluid velocities. (Anonymous, 2022f)

$$Re: \frac{Ud}{\nu}$$

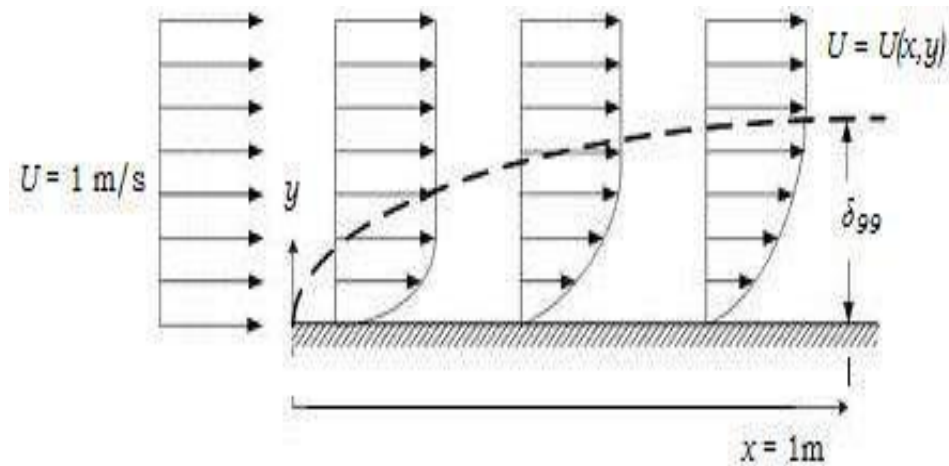


Figure 2.5. Boundary Layer Thickness On Flat Plate.(Anonymous, 2022 f)

The calculated Reynolds number determines the shape of the flow. If the Reynolds number is;

- If $Re < 2000$, the flow is laminar;
- If $2000 \leq Re \leq 4000$, the flow is laminar or turbulent.
- If $Re > 4000$, the flow is turbulent.

2.2.1.2.2. Mach Number

The most important criterion in considering compressibility in aerodynamics is the Mach number. Mach number is a dimensionless parameter, u is equal to the ratio of the velocity of the fluid and α of the speed of sound in the medium. (Sadraey, 2013)

$$M: \frac{u}{\alpha}$$

The speed of sound is essentially the speed of propagation of any disturbance or, in other words, pressure wave that occurs in the flow field.(Sadraey, 2013)

2.3. Airfoils Aerodynamics

2.3.1. General Features of an Airfoil

Profile geometry is a geometry that exists in nature and produces very efficient results in terms of aerodynamics. The two-dimensional cross-section view of the three-dimensional wing of the aircraft, which is the most widely used among aircraft, in the x-z plane, according to the previously defined axis set, is called the airfoil. The shape of the airfoil is of vital importance, and this shape has a leading role in the formation of all forces and moments. (Sadraey, 2013)

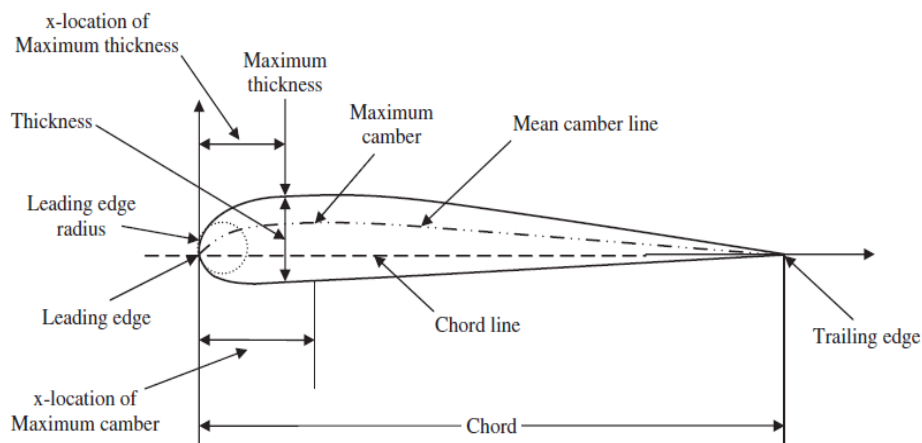


Figure 2.6. Airfoil geometric parameters (Sadraey, 2013)

We can observe the representations of the basic profile parameters on the figure from the picture above. Accordingly, the front part of the profile is called the leading edge, and the rear part is called the trailing edge. The shortest linear distance between these two edges is called the chord line. Line segments connecting the leading edge and trailing edge of the profile and joining the points of the upper surface and lower surface within the same vertical axis are called the profile thickness, and the curve obtained when the midpoints of these segments are combined is called the camber curve. The distance of the camber curve from the chord line is defined as camber. The ratio of the maximum thickness of the profile to the length of the chord is called the maximum thickness ratio, and the ratio of the maximum camber to the chord line is called the maximum camber ratio. In order to indicate the curvature of the leading edge, the radius of the circle, which is generally thought to pass tangentially from the

leading edge, is taken into account and this value is called the leading-edge radius.(Sadraey, 2013)

2.3.2. NACA Airfoils

NACA airfoils are airfoil shapes for aircraft wings developed by the National Advisory Committee for Aeronautics (NACA). The shape of NACA airfoils is described using a series of numbers following the word "NACA". Parameters in numerical code can be entered into equations to precisely construct the cross section of the airfoil and calculate its properties.

The development of NACA profiles dates back to the 1930s. Especially the Langley research center in the US state of Virginia and the wind tunnels in this center have historical importance and memories in terms of scientific studies on airfoils. In the light of the data obtained because of hundreds of wind tunnel experiments on tens of profiles at the NACA Langley research center, we see that different systematic approaches have been developed to produce profile geometry. The first of these approaches is profile and geometry definition with 4, 5 or 6 digit numbers.(Sadraey, 2013)

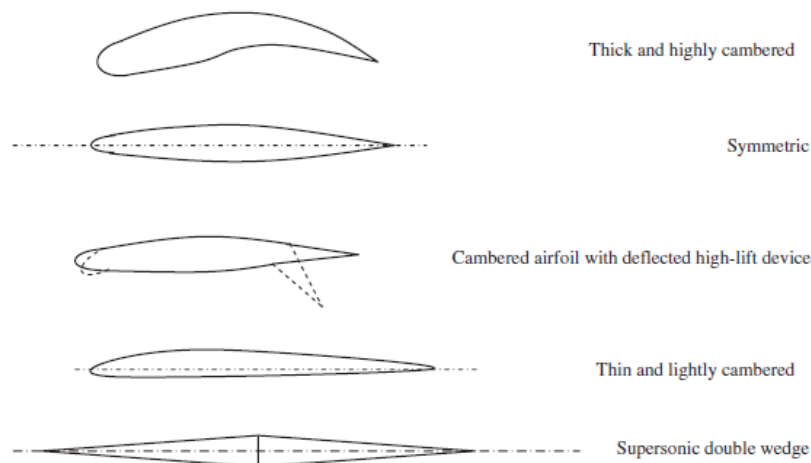


Figure 2.7. Five sample airfoil sections (Sadraey, 2013)

2.3.2.1. Four-Digit NACA Airfoils

The four-digit NACA airfoil is the oldest and simplest NACA profile to manufacture. The camber of a four-digit airfoil consists of two parabolas. One parabola produces the camber geometry from leading edge to maximum camber, and another parabola produces the camber shape from maximum camber to trailing edge. (Sadraey, 2013)

2.3.2.2. Five-Digit NACA Airfoils

The camber of a five-digit airfoil section is made up of one parabola and one straight line. The parabola generates the camber geometry from the leading edge to the maximum camber, and then a straight line connects the end point of the parabola to the trailing edge. (Sadraey, 2013)

2.3.2.3. The 6-Series NACA Airfoils

The 6-series NACA airfoils are designated by five main digits and begin with the number 6. Some 6-series airfoils have a subscript number after the second digit. There is also a “-” between the second digit and the third digit. (Sadraey, 2013)

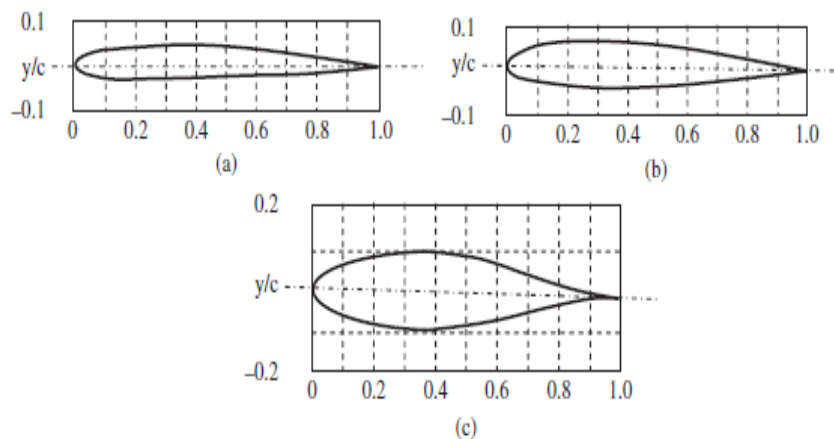


Figure 2.8. Four-digit, a five-digit, and a 6-series airfoil section: (a) NACA 1408; (b) NACA 23012; and (c) NACA 633-218. (Sadraey, 2013)

3. MATERIAL AND METHOD

3.1. Preliminary Design

Before starting the design, it is necessary to determine the design criteria that will shape our design. These design criteria are the most important criteria for the purpose of use of the UAV that we will design. All other features are determined according to the purpose of use. We can summarize the purpose of the UAV as follows.

- Ensuring the environmental safety of industrial facilities.
- Fire detection in forest areas and alerting relevant units.
- Three-dimensional modeling of the land with addable advanced camera and scanning systems.
- Ensuring the environmental security of agricultural lands.
- Contributing to search and rescue processes in environmental disasters.
- Providing condition-damage assessment in environmental disasters.
- Since the UAV can be pre-programmed to fulfill its tasks such as environmental security (periodic time, flight altitude, etc.), it will not need a remote-control system.
- Does not need to inform the control center unless a problem is detected during the patrol flight. Informing the relevant units about this issue when faced with a negative situation. That is, the UAV will have an active-passive system.
- Flight speed will be below mach speed.
- Airtime will be at most one hour.

As a result, my thesis advisor Prof.Dr. İsmail BÖREKÇİ, we decided to make vertical take-off and landing with three engines and wings. After determining the design criteria, it was time to determine their mechanical properties. In order to determine these mechanical and physical properties, we examined the characteristics of previously produced vertical take-off UAVs and winged UAV.

By examining the physical and mechanical parameters (W_{TO} , S_W (S_{Ref}), V_{Max} , h_{Max} , b , etc..) of the examined UAVs, we made some preliminary assumptions for our UAV. Using these presuppositions, some theoretical values were calculated. It should be noted that the assumptions made are not fixed. The values for optimization may change according to the results of the analysis made in the computer environment after the design is completed.

The technical specifications of some models examined as technical reviews are given below.



Figure 3.1. Akıncı TİHA (Anonymous, 2022 g)

Akıncı TİHA Technical Specifications

Crew: none

Length: 12.2 m (40 ft)

Wingspan: 20.0 m (65.6 ft)

Height: 4.1 m (13.1 ft)

Maximum take-off weight: 5500 kg (12,125 lb.)

Payload: 1,500 kg (3,300 lb.)

Internal: 450 kg (990 lb.)

External: 900 kg (2,000 lb.)

Power unit: 2× IvchenkoH-Progress AI-450C turboprop engine, 450 hp (335 kW)
(Each)

Performance

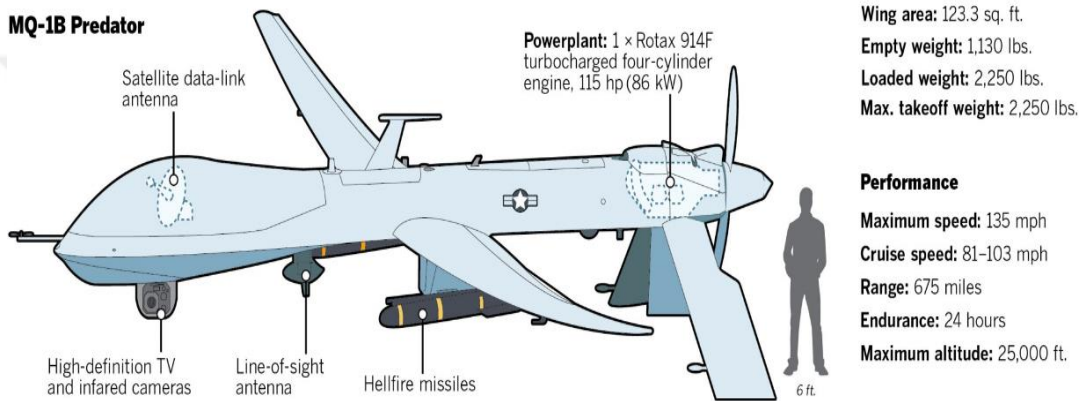
Maximum speed: 195 knots (361 km/h)

Service ceiling: 40,000 feet (12,192 m)

Spy in the sky

San Diego's General Atomics revolutionized modern warfare by developing Predator, a remotely operated unmanned aerial system, or drone, capable of staying in the sky for hours, conducting surveillance and reconnaissance and sharing live videos with other parties. The plane also was fitted with Hellfire missiles. Predator was succeeded by a larger, more robust drone known as Reaper.

MQ-1B Predator



Sources: General Atomics; U.S. Air Force

MICHELLE GUERRERO U-T

Figure 3.2. The Predator USA (Anonymous, 2022h)



Figure 3.3. Delta Quad Pro (D. Raymer ,2018)

Wingspan:	235 cm
Length:	90 cm
Wing area:	90 sq. dm.
Empty weight:	3.3 Kg
Empty weight including battery:	5 Kg
Maximum takeoff weight:	6.2 Kg
Payload capacity:	1.2 Kg
Cruise speed:	18 m/s (65 Km/h)
Maximum speed:	28 m/s (100 Km/h)
Stall speed:	12 m/s (43 Km/h)

Total take-off weight, wingspan, length values, aspect ratios ($AR=b^2/S$), wing loading (W/S) of the examined models were calculated. According to these calculations, the weight, wing length and wing area values of our model were estimated. In addition, the aspect ratio was compared with the values accepted in the literature (Figure 5.3).

No.	Aircraft type	Aspect ratio
1	Hang glider	4–8
2	Glider (sailplane)	20–40
3	Home-built	4–7
4	General aviation	5–9
5	Jet trainer	4–8
6	Low-subsonic transport	6–9
7	High-subsonic transport	8–12
8	Supersonic fighter	2–4
9	Tactical missile	0.3–1
10	Hypersonic aircraft	1–3

Figure 3.4. Typical values of wing aspect ratio (D. Raymer ,2018)

The predicted values before proceeding to the calculations are given in the table below.

Table 3.1. Assumptions to be used in theoretical calculations

Crew	No	Unit
Wingspan	1,614	m
Max Cruise Height	5000	m
Maximum Take-Off Weight	15	kg
Cruise Speed	18	m/sn
Max Speed	20	m/sn
Per RC Motor Thrust	7	kg
Per Motor Average RPM	5040	rpm
RC Motor Numbers	3	
Sweep angle	0	deg
Wing Reference Area	0,5	m ²

Table 3.2. Formulas used with calculated values

	Formula	Description	Symbols	Value	Result	Unit
1	$T_u = T_o - \lambda * h$ (kelvin)	Altitude Temperature Change	Sea Level Temperature= T_o (kelvin)	288	255,50	kelvin
			Coefficient values of temperature change= λ	-6,5		
			Max Height= h (km)	5		
2	$\rho_u = \rho_o(1 - (h/44308))^{4.259}$	Altitude air density change	Sea Level Density= ρ_o (kg/m ³)	1,2267	0,736656891	(kg/m ³)
			Max Height= h (m)	5000		
3	$\mu_u = \mu_o(T_u/T_o)^{0.75}$	Altitude dynamic viscous change	Absolute Viscosity= μ_o (kg/ms)	$1,710 \times 10^{-5}$	$1,563 \times 10^{-5}$	kg / m sn
			Sea Level Temperature= T_o (kelvin)	288		
			Altitude Temperature Change= T_u (kelvin)	255,50		
4	$Re = \rho_u VL / \mu$	Reynolds Number	Altitude Air Density Change= ρ_u (kg / m sn)	1,225	1.796.117,785	Unitless
			True Airspeed= V_{Tip} (m/sn)	76,4		
			Flow Contact Length = L (m)	0,3		
			Altitude dynamic viscous change= μ_u	$1,563 \times 10^{-5}$		
5	$AR = b^2/S$	Aspect Ratio	Wingspan= b (m)	1,614	7,623823529	Unitless
			Wing Reference Area= S (m ²)	0,340		
6	$M = V_{Tip}/c$	Mach Number	True Airspeed = V_{Tip} (m/sn)	76,396	0,222599976	Mach
			Speed of sound: c (m/sn)	343,200		
7	$q_o = 1/2 * \rho_o * V^2$	dynamic pressure	Sea Level Density= ρ_o (kg/m ³)	1,227	3.579,754	kgf/m ²
			True Airspeed= V_{Tip} (m/sn)	76,4		

Table 3.2. Formulas used with calculated values (more)

8	$Cl=(2*L)/(pV^2S)$	The Lift Coefficient	Lifting Force=L(N)	150	0,093245497	Unitless
			True Airspeed = $V_{Tip}(m/sn)$	76,4		
			Sea Level Density= ρ_0 (kg/m ³)	1,2250		
			Referance Wing Surface Area=S (m ²)	0,45		
9	$D=Cd*1/2*\rho_0*V^2*S$	Drag Force	Drag Coefficient=Cd	0,00144	2,577422714	Newton
			Sea Level Density = ρ_0 (kg/m ³)	1,2267		
			True Airspeed = $V_{Tip}(m/sn)$	76,4		
			Referance Wing Surface Area = S (m ²)	0,5		
10	$M=Cm*1/2*\rho_0*V^2*S$	Pitch moment	Pitch Moment Coefficient = Cm	-0,04130	68,00816211	Newton
			Sea Level Density= ρ_0 (kg/m ³)	1,2267		
			True Airspeed = $V_{Tip}(m/sn)$	76,4		
			Referance Wing Surface Area = S (m ²)	0,46		
11	T/W	Thrust Value Per Unit Weight	Thrust Force = T = D(N)	0,00144	0,0000096	Unitless
			Weight = W(N)	150		
12	$(V_{tip})_o = \pi n D a / 60$	Air Velocity At The Tip Of The Propeller	RC Motor Spedd=n (rpm)	5040	73,73192294	m/sn
			Propeller Diameter=D (m)	0,2794		
			Number of RC motor=a	1		
13	$V_{tip} = ((V_{tip})_o^2 + V_{\infty}^2)^{1/2}$	True Airspeed	Air Velocity At The Tip Of The Propeller= $(V_{tip})_o$ (m/sn)	73,73192	76,39631183	m/sn
			Max Speed= V_{∞} (m/sn)	20,0		
14	$V_{stall} = ((2*(W/S)/(p*Cl))^{1/2})$	Stall Speed	Weight = W(kg)	15	16,72289788	m/sn
			Wing Referance Area=S(m ²)	0,5		
			The Lift Coefficient=Cl	0,17490		
			Sea Level Density = ρ_0 (kg/m ³)	1,2267		
15	$\lambda = c_t / c_r$	Taper Ratio	Tip Chord= c_t (m)	0,086	0,306049822	Unitless
			Root Chord = c_r (m)	0,281		

3.2. Wing Design

3.2.1. Number Of Wing

In the past, the most logical way to increase flight safety was to increase the number of wings, since production technologies were not developed much and the quality of the materials used was poor.

Today, with the developing technology, Almost all modern aircraft today have monoplanes.(D. Raymer ,2018)

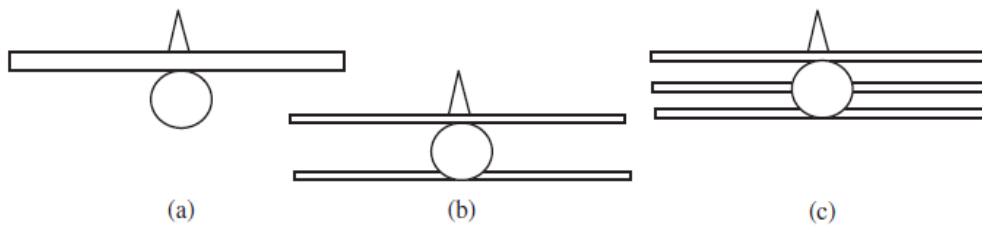


Figure 3.5. Three options in number of wings (front view): (a) Monoplane; (b) Biplane; and (c) Tri-wing (D. Raymer ,2018)

The UAV, which we designed, has monoplane wing. The reason we use a monoplane wing is that it is completely monoplane in both UAV models and all types of aircraft used. Also, the fact that it is a single wing is also important in terms of the weight of our UAV.

3.2.2. Wing Vertical Location

One of the wing parameters that can determine the wing design process is the position of the wing relative to the fuselage. There are four different accepted designs for the position of the wing.

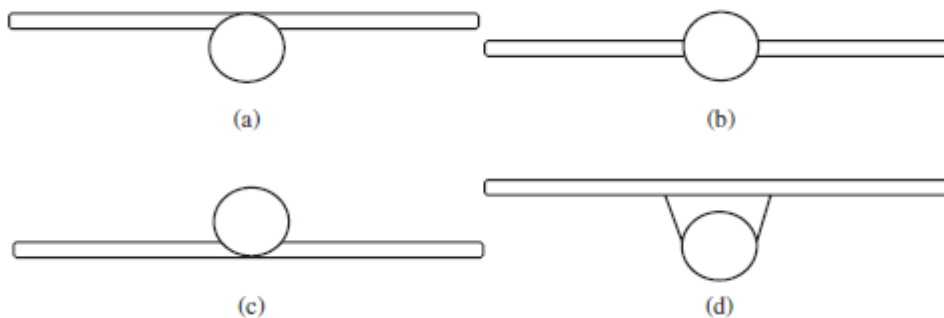


Figure 3.6. Options in vertical wing positions: (a) High wing; (b) Mid-wing; (c) Low wing; and (d) Parasol wing



Figure 3.7. Four aircraft with different wing vertical positions: (a) Lockheed Martin C-130J Hercules (high wing); (b) Boeing 767 (low wing); (c) Pietenpol Air Camper-2 (parasol wing); (d) Hawker Sea Hawk (mid-wing)

Each of the above-mentioned positioning types has advantages and disadvantages relative to each other. In our research, we decided that the wing location of our model should be low.

3.2.3. Airfoil Section

An airfoil is a structure designed to produce lift and drag forces when moved in air. In the process of wing airfoil selection, there are several graphs that illustrate the characteristics of each airfoil when compared to other airfoils. These are mainly the variations of non-dimensionalized lift, drag, and pitching moment relative with angle of attack.

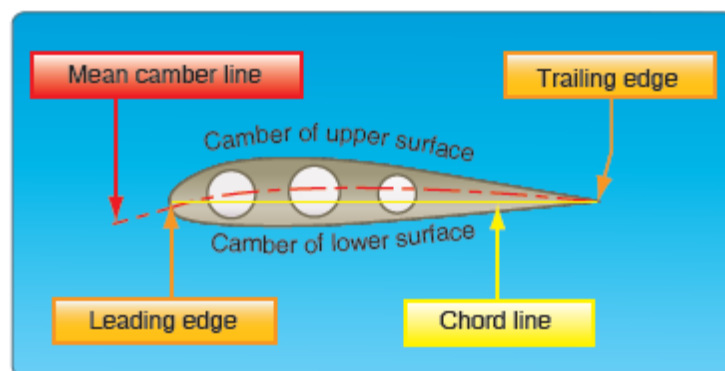


Figure 3.8. Typical airfoil section (U.S. Department of Transportation Federal Aviation Administration Flight Standards Service, 2016)

Designing a new airfoil that has never been tried is a complex and time-consuming process. In addition, advanced aerodynamic fundamentals are required for airfoil design. It is also a costly process in which the newly designed airfoil needs to be tested and verified in wind tunnels. It is useful to use the profile types tested and published by research centers such as Airbus, Boeing companies and the National Advisory Committee for Aeronautics (NACA).

We need to add some parameters in addition to the values we calculated in section 5 without selecting these NACA profiles.

3.2.3.1. The Wing Maximum Thickness To-Chord Ratio;

In wing profiles, the thickness is the distance between the upper and lower points of the profile. It is not given as a direct measurement in the profile selection. The ratio of the thickness to the chord length is called the thickness ratio and is determined as a percentage. In general, the maximum thickness ratio of the profile is determined, and it is called “ t_{\max}/c ” ratio.

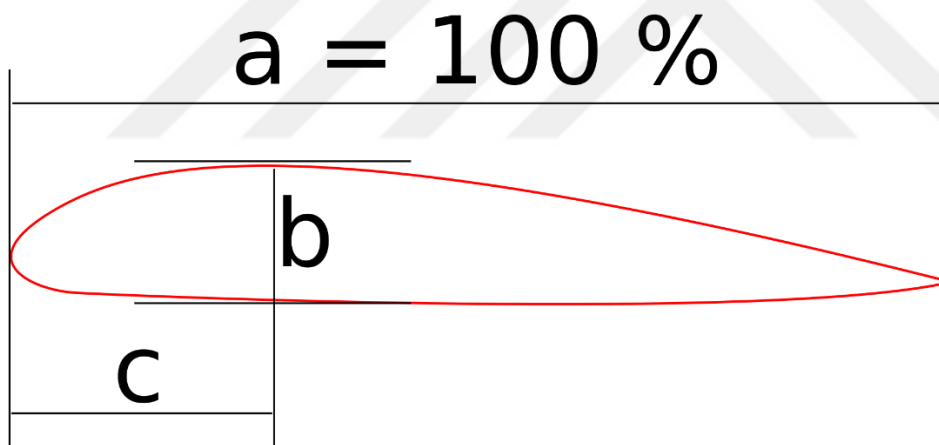


Figure 3.9. The Wing Maximum Thickness To-Chord Ratio.

As a guide, typical values for the airfoil maximum thickness-to-chord ratio of the majority of aircraft are about 6–18%.(U.S. Department of Transportation Federal Aviation Administration Flight Standards Service, 2016)

1. the typical wing $(t/c)_{\max}$ of cargo aircraft is about 15-18%
2. The typical wing $(t/c)_{\max}$ of high subsonic passenger aircraft is about 9–12%.
3. The typical wing $(t/c)_{\max}$ of supersonic aircraft is about 3–9%.

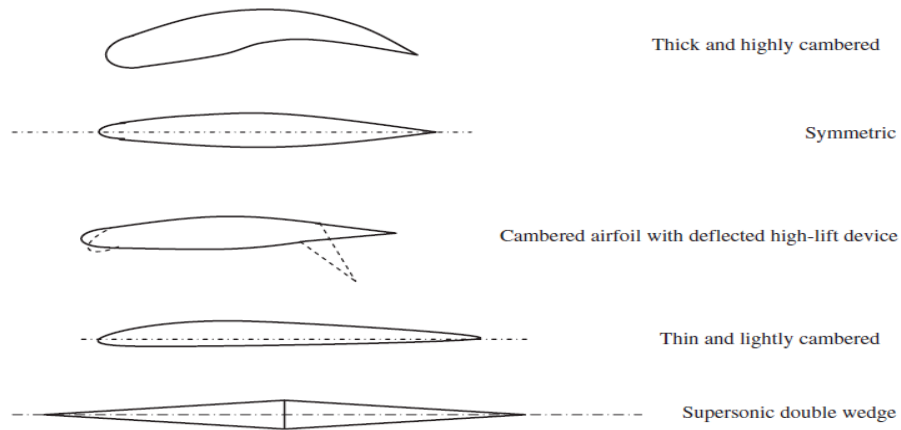


Figure 3.10. Five sample airfoil sections (U.S. Department of Transportation Federal Aviation Administration Flight Standards Service, 2016)

Since the UAV we will design will fly at speeds below the speed of sound, profiles with a thickness ratio equal to 14% and large will be examined.

3.2.3.2. The Angle Of Attack

Angle of attack is the angle between the wing chord line and the free flow direction towards the profile. The effect of this value on the formation of aerodynamic forces is quite large. Because it is the only factor that determines how the flow and thus the fluid interacts with the profile geometry.(U.S. Department of Transportation Federal Aviation Administration Flight Standards Service, 2016)

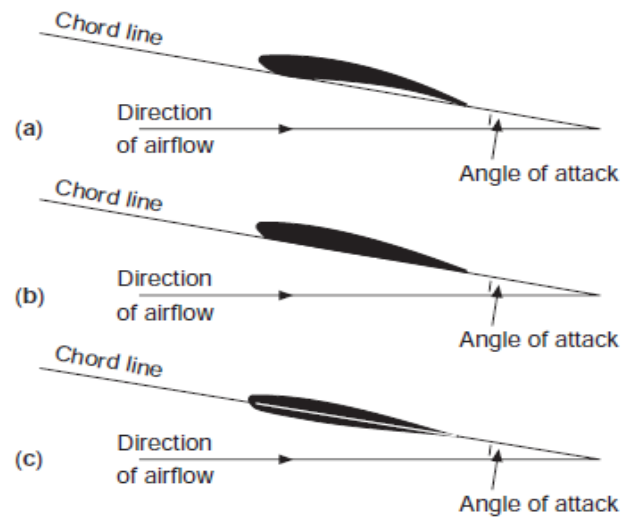


Figure 3.11. Chord line and angle of attack (a) Aerofoil with concave undersurface. (b) Aerofoil with flat undersurface. (c) Aerofoil with convex undersurface. (Kermode, et al., 2006)

The critical angle for most airfoils is 15° . However, this value can be increased thanks to additional aerodynamic surfaces, warplanes are the aircraft with the highest capacity in this regard; Angles of attack can vary between 20° and 45° . In some designs, this value can even reach 90° .

The angle of attack is directly proportional to the lift force. As the angle of attack increases, the lift force increases, but if the angle exceeds the critical value (20°), the drag force increases accordingly. The increase in drag force makes it difficult for the aircraft to hold in the air.

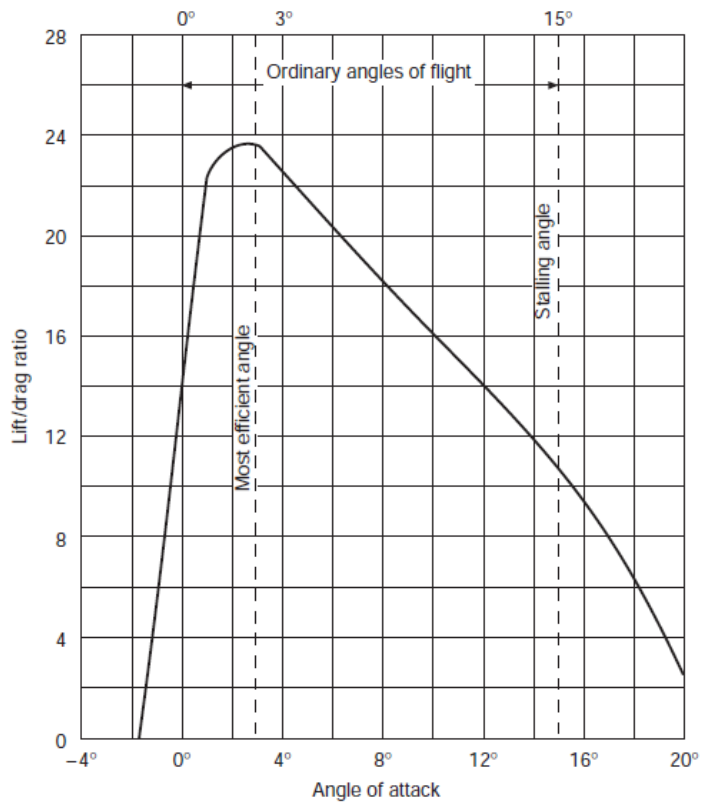


Figure 3.12. Lift/drag curve (Kermode, et al., 2006)

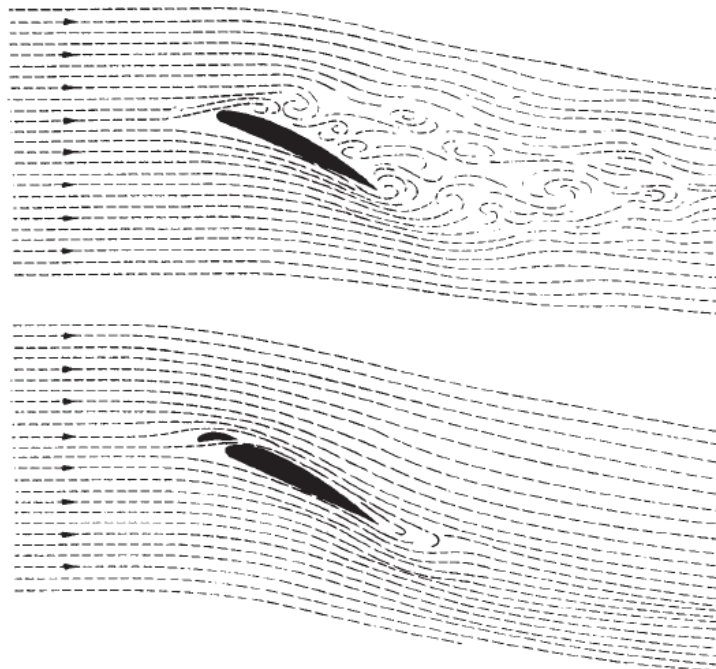


Figure 3.13. Effect of slot on airflow over an airfoil at large angle of attack (Kermode, et al., 2006)

3.2.3.3. Swept Wing

The swept wing is a type of wing used in high-speed aircraft and got its name from the way the wings look like arrows when viewed from above, with the tips of the wings pulled back. While retracted wings express the backward arrow angle, airplanes with forward swept wings have also been seen in history. The reason for the existence of swept wings is the behavior of air at a speed close to the speed of sound on the airfoil.

The swept wings are common on aircraft that perform some of their flight at near the speed of sound, such as jets, business jets, and commercial airplanes, usually fighter jets. The main reason for setting the arrow angle is to increase the critical mach number. The critical Mach number is the speed of the aircraft when the air traveling at speeds close to the speed of sound accelerates on the upper surface of the airfoil and reaches the speed of sound. An oblique shock wave is seen on the wing of an airplane traveling at a critical mach number. This, as one of the reasons that increases drag, can cause both more fuel consumption and wing strain or loss of control due to the jolts it creates during flight. (Kermode, et al., 2006)

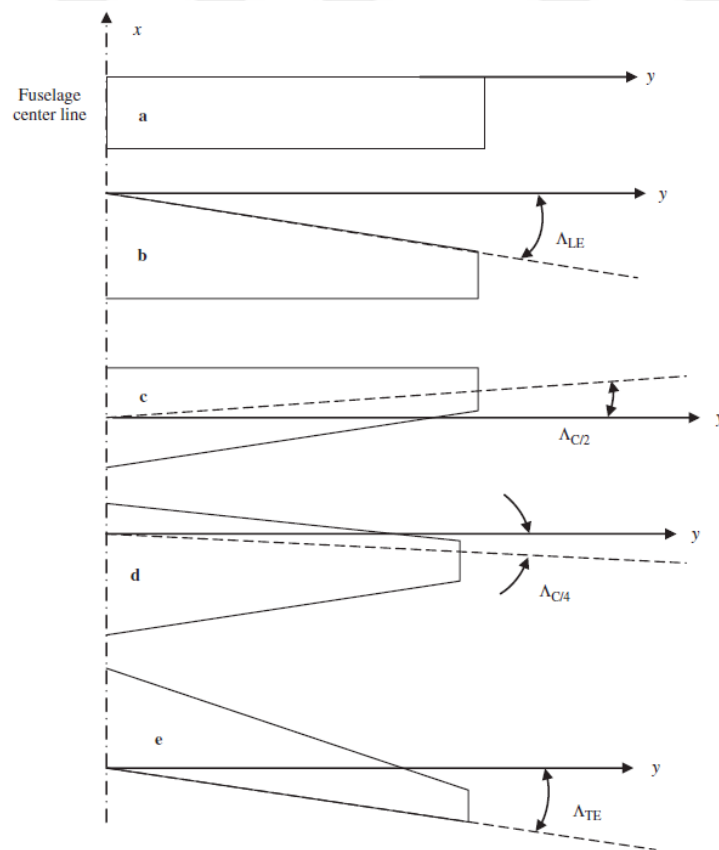


Figure 3.14. Five wings with different sweep angles (Kermode, et al., 2006)

Since our UAV model will move below the speed of sound, the swept wing is assumed to be zero. ($\Lambda = 0^\circ$).

3.2.3.4. Dihedral Angle

When we look at an airplane from the front, we see that the wings make an angle with the horizontal. This angle is called the dihedral angle. If we accept the ground as a reference; if the wing tip is moving away from the ground, it is called a positive dihedral angle, if it is parallel, it is called a zero-dihedral angle, if it is approaching the ground, it is called a negative (anhedral) dihedral angle. The purpose of the dihedral angle is to increase aerodynamics.

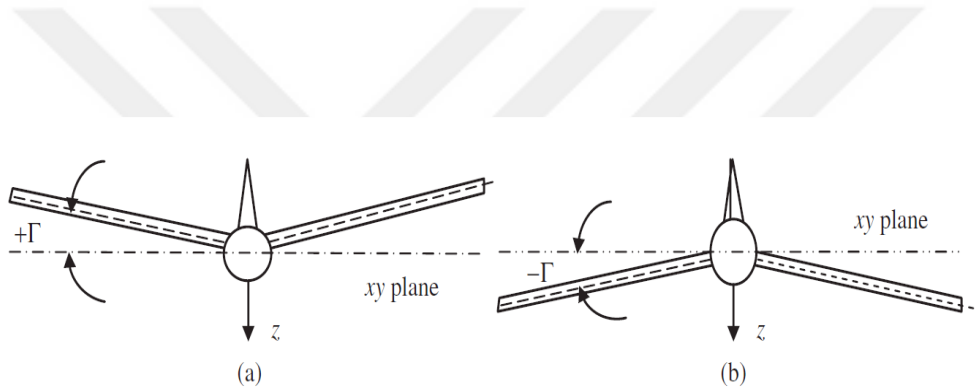


Figure 3.15. (a) Dihedral and (b) anhedral (aircraft front view) (Kermode, et al., 2006)

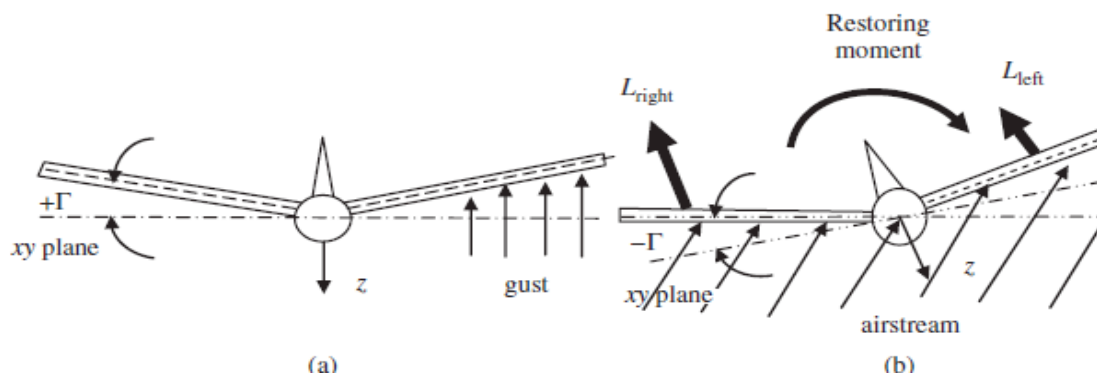


Figure 3.16. The effect of dihedral angle on a disturbance in roll (aircraft front view): (a) before gust; (b) after gust. (Kermode, et al., 2006)

Table 3.3. Determination of the dihedral angle

	Wing Vertical Location		
	Low Wing	Mid-Wing	High Wing
$\Lambda=0$	5 - 7	2 - 4	0 - 2
Subsonic Swept Wing	3 - 7	-2 - 2	-5 - -2
Supersonic Swept Wing	0 - 5	-5 - 0	-5 - 0

The recommended angle value for the low wing non-swept wing is 5-7 degrees. We determined this angle as 6 degrees in our design.

3.2.3.5. Camber Ratio

A camber curve is created by combining the points in the middle of the lower and upper points of the wing profiles. The distance from the point where the maximum camber occurs to the root line gives the camber value. The ratio of the place where this value is maximum to the length of the vet will give the maximum camber ratio. The camber ratio is denoted by γ . The camber ratio takes values greater than or equal to zero. When it is less than zero, the airfoil creates a pressure difference opposite to the desired one in the upper and lower parts of the airfoil and causes the airfoil to not fulfill its function. When the camber ratio is equal to zero, the wing is called a symmetrical wing. In the selection of airfoils, the maximum camber ratio (γ_{Max}) recommended for aircraft is specified in the literature.(17)

✓ The γ_{Max} range of 0-5% is called the small camber ratio and is used in aircraft at these ratios.

✓ The γ_{Max} is in the range of 8-12%, it is called high camber ratio, it is used in compressors and turbines.

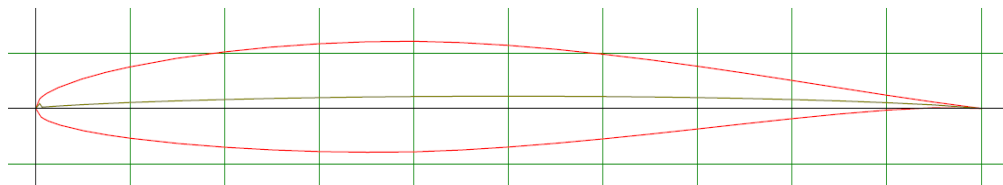
Since the UAV we will design is an aircraft, the maximum chord ratio will be selected in the range of 0-5%.

3.3. Wing Airfoil Section Selection

The purpose of all our assumptions and calculations we have made so far was to select the ideal wing airfoil. For the profile selection, NACA profiles will be selected by considering

the values close to the wing thickness and the chord ratio, plus the lift coefficient, the Reynolds number, and the Mach number.

As a result of our research, we decided to use the NACA 64210 profile as the airfoil.



Details
 (naca64210-il) NACA 64-210
 NACA 64-210 airfoil
 Max thickness 10% at 40% chord.
 Max camber 1.1% at 50% chord

Figure 3.17. NACA 64210 (Melin, 2013)

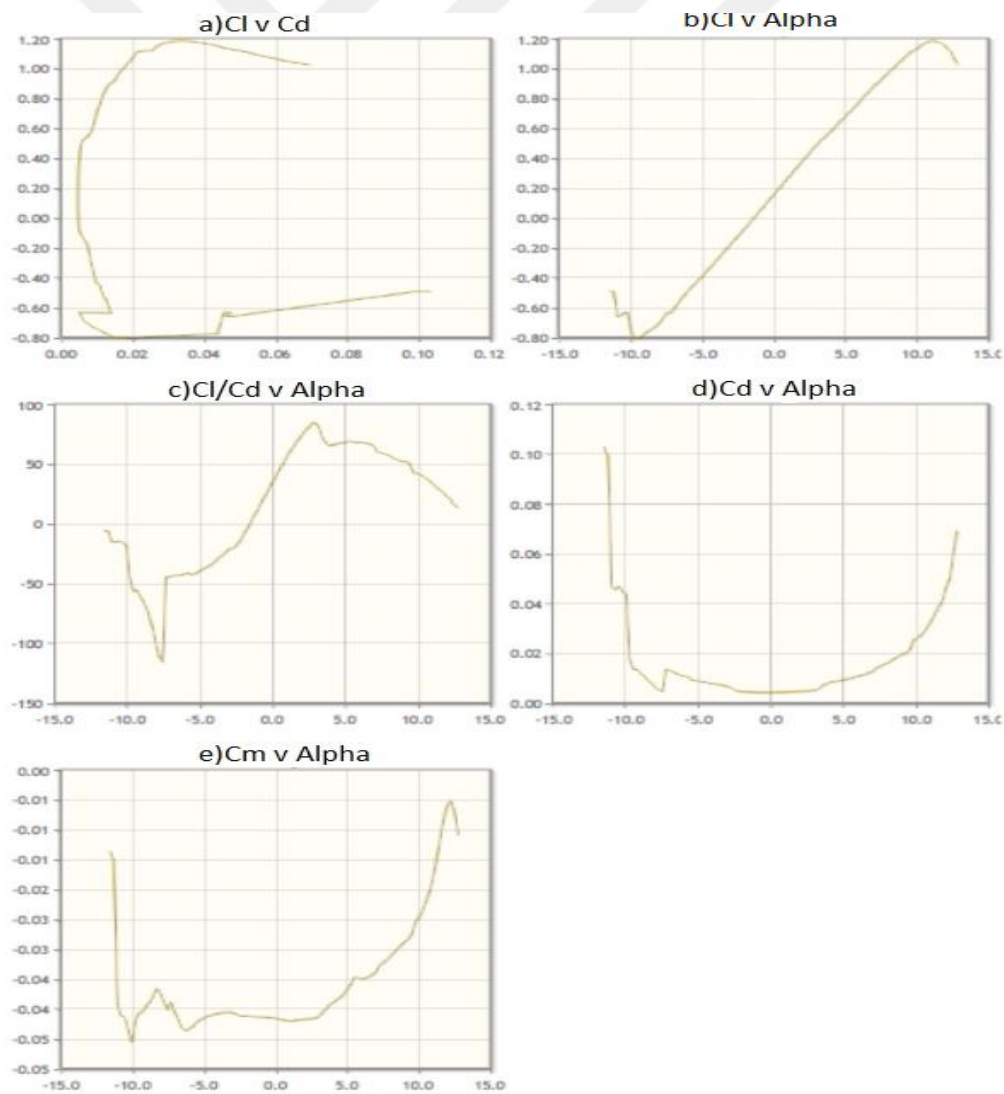


Figure 3.18. Aerodynamic coefficient graphs. a) The variations the lift coefficient versus of the drag coefficient. b) The variations of lift coefficient versus the angle of attack. c) The variations of the lift-to-drag ratio versus the angle of attack. d) The variations of drag coefficient versus the angle of attack. e) The Variations of Pitching Moment Coefficient versus Angle of Attack.(Melin, 2013)

When the graph between the lift coefficient and the alpha is examined, the lift force increases linearly as alpha increases. We accepted angle of incidence is zero degrees. Again, the number of drag coefficient corresponding to the zero angle in the graphs is at a minimum level. Again, when we examine the relationship between the pitching moment coefficient and the alpha, the C_m coefficient is minimum when the angle of attack is zero. Considering all these results, the NACA profile we have chosen for the wing is the right choice.

Table 3.4. Table of coefficients for NACA 64210 depending on the changing angle of attack (Melin, 2013)

Alpha	Cl	Cd	Cdp	Cm	Alpha	Cl	Cd	Cdp	Cm
-11.500	-0.4820	0.10340	0.10186	-0.0134	0.750	0.2598	0.00512	0.00097	-0.0416
-11.250	-0.4806	0.09944	0.09790	-0.0149	1.000	0.2880	0.00514	0.00099	-0.0417
-11.000	-0.6490	0.04728	0.04569	-0.0390	1.250	0.3161	0.00519	0.00103	-0.0417
-10.750	-0.6411	0.04610	0.04449	-0.0408	1.500	0.3438	0.00523	0.00106	-0.0416
-10.500	-0.6221	0.04768	0.04610	-0.0411	1.750	0.3712	0.00532	0.00109	-0.0415
-10.250	-0.6224	0.04558	0.04396	-0.0430	2.000	0.3989	0.00540	0.00114	-0.0415
-10.000	-0.7614	0.04400	0.04192	-0.0453	2.250	0.4263	0.00549	0.00121	-0.0414
-9.750	-0.7926	0.01828	0.01543	-0.0419	2.500	0.4538	0.00559	0.00128	-0.0414
-9.500	-0.7942	0.01441	0.01122	-0.0405	2.750	0.4813	0.00570	0.00136	-0.0413
-9.250	-0.7736	0.01419	0.01099	-0.0402	3.000	0.5075	0.00592	0.00148	-0.0411
-9.000	-0.7582	0.01274	0.00938	-0.0394	3.250	0.5310	0.00656	0.00170	-0.0405
-8.750	-0.7423	0.01125	0.00770	-0.0386	3.500	0.5521	0.00759	0.00213	-0.0398
-8.500	-0.7250	0.01006	0.00636	-0.0377	3.750	0.5742	0.00844	0.00252	-0.0392
-8.250	-0.7102	0.00854	0.00463	-0.0363	4.000	0.5981	0.00900	0.00286	-0.0387
-8.000	-0.6834	0.00710	0.00295	-0.0372	4.250	0.6235	0.00931	0.00313	-0.0383
-7.750	-0.6540	0.00597	0.00163	-0.0385	4.500	0.6490	0.00955	0.00341	-0.0379
-7.500	-0.6219	0.00543	0.00095	-0.0399	4.750	0.6737	0.00985	0.00373	-0.0373
-7.250	-0.6249	0.01435	0.00940	-0.0385	5.000	0.6979	0.01014	0.00411	-0.0366
-7.000	-0.5911	0.01370	0.00873	-0.0403	5.250	0.7215	0.01036	0.00438	-0.0357
-6.750	-0.5589	0.01320	0.00820	-0.0416	5.500	0.7433	0.01065	0.00471	-0.0345
-6.500	-0.5268	0.01255	0.00747	-0.0428	5.750	0.7700	0.01119	0.00535	-0.0344
-6.250	-0.4974	0.01193	0.00677	-0.0434	6.000	0.7981	0.01154	0.00574	-0.0348
-6.000	-0.4713	0.01149	0.00626	-0.0431	6.250	0.8240	0.01197	0.00621	-0.0346
-5.750	-0.4456	0.01121	0.00590	-0.0427	6.500	0.8494	0.01243	0.00670	-0.0344
-5.500	-0.4232	0.01020	0.00477	-0.0420	6.750	0.8744	0.01292	0.00721	-0.0341
-5.250	-0.3977	0.00986	0.00438	-0.0416	7.000	0.8986	0.01349	0.00781	-0.0337
-5.000	-0.3718	0.00957	0.00402	-0.0413	7.250	0.9171	0.01493	0.00935	-0.0325
-4.750	-0.3456	0.00930	0.00368	-0.0410	7.500	0.9411	0.01554	0.01002	-0.0321
-4.500	-0.3187	0.00909	0.00342	-0.0408	7.750	0.9650	0.01616	0.01070	-0.0316
-4.250	-0.2926	0.00862	0.00285	-0.0406	8.000	0.9882	0.01691	0.01152	-0.0311

-4.000	-0.2657	0.00841	0.00261	-0.0405	8.250	1.0108	0.01776	0.01246	-0.0304
-3.750	-0.2382	0.00826	0.00241	-0.0404	8.500	1.0332	0.01864	0.01342	-0.0298
-3.500	-0.2111	0.00797	0.00208	-0.0403	8.750	1.0553	0.01955	0.01441	-0.0292
-3.250	-0.1836	0.00780	0.00187	-0.0403	9.000	1.0776	0.02029	0.01523	-0.0286
-3.000	-0.1564	0.00747	0.00166	-0.0403	9.250	1.0999	0.02083	0.01579	-0.0282
-2.750	-0.1304	0.00678	0.00140	-0.0405	9.500	1.1200	0.02180	0.01683	-0.0274
-2.500	-0.1052	0.00578	0.00111	-0.0408	9.750	1.1282	0.02588	0.02129	-0.0254
-2.250	-0.0781	0.00542	0.00103	-0.0409	10.000	1.1478	0.02660	0.02215	-0.0245
-2.000	-0.0504	0.00530	0.00098	-0.0409	10.250	1.1649	0.02778	0.02349	-0.0234
-1.750	-0.0222	0.00522	0.00094	-0.0410	10.500	1.1791	0.02934	0.02523	-0.0220
-1.500	0.0059	0.00518	0.00090	-0.0410	10.750	1.1888	0.03143	0.02756	-0.0202
-1.250	0.0340	0.00513	0.00089	-0.0411	11.000	1.1933	0.03393	0.03032	-0.0180
-1.000	0.0619	0.00507	0.00090	-0.0411	11.250	1.1895	0.03673	0.03338	-0.0149
-0.750	0.0898	0.00506	0.00091	-0.0411	11.500	1.1801	0.03924	0.03611	-0.0112
-0.500	0.1182	0.00505	0.00091	-0.0412	11.750	1.1675	0.04212	0.03920	-0.0082
-0.250	0.1466	0.00506	0.00091	-0.0412	12.000	1.1399	0.04697	0.04435	-0.0057
0.000	0.1749	0.00507	0.00091	-0.0413	12.250	1.1232	0.05089	0.04845	-0.0050
0.250	0.2033	0.00508	0.00093	-0.0414	12.500	1.0678	0.06087	0.05880	-0.0067
0.500	0.2315	0.00511	0.00094	-0.0415	12.750	1.0312	0.06962	0.06778	-0.0107

3.3.1. Wing 3D Model Design

3D design of the wing; After determining the wing airfoil, dimensions and angle of attack, it was made in line with these data. We will use SolidWorks as the design program.

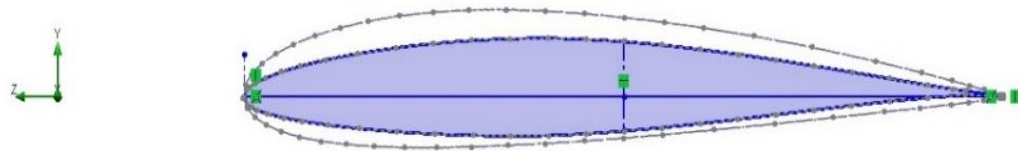


Figure 3.19. NACA 64210 airflows

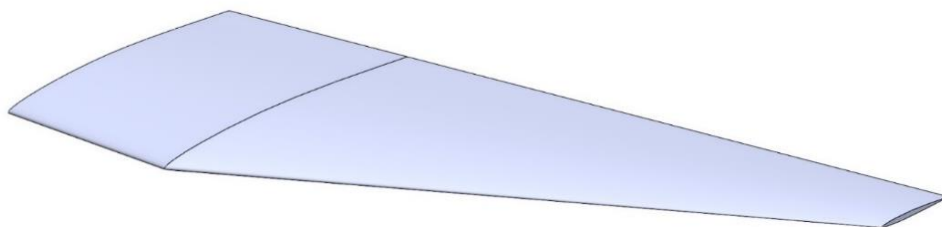


Figure 3.20. 3D Model Wing

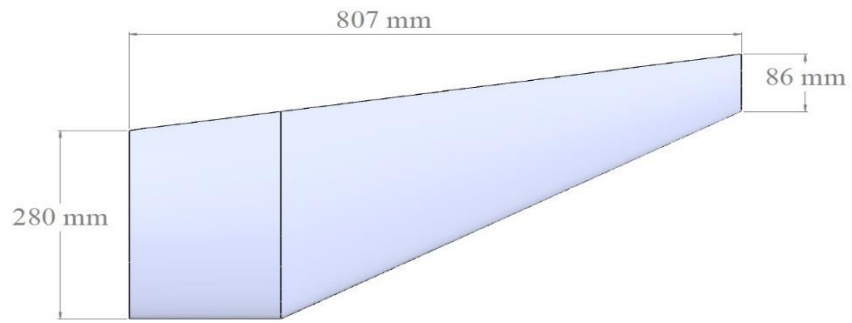


Figure 3.21. Wing Dimensions (root chord, tip chord, wingspan)

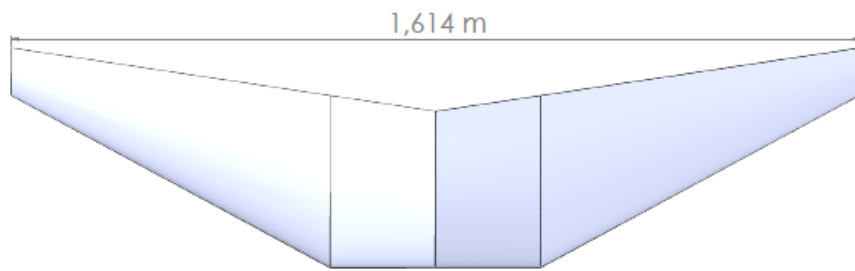


Figure 3.22. Left, Right Wing (total wingspan)

3.4. Fuselage Design

3.4.1. Fuselage Airfoil Section Selection

The most important part of an aircraft is the fuselage. Because it contains all the useful loads. The UAV's control cards, camera and camera systems, must be in the required volume to carry important components such as gps cards and the center of gravity of the equipment must be adjusted appropriately for balancing. The geometry of the fuselage is the wing geometry. It must be compatible with the aircraft and must not cause adverse aerodynamic effects during flight.

Instead of designing the fuselage geometry from scratch, we used NACA profiles as in the wings. Because, as it is known, NACA profiles enter the literature after the necessary tests are completed, so we do not take unnecessary risks in use. Unlike the wing profile, considering the components that the fuselage profile will carry, the $(t/c)_{max}$ value is 14%. The NACA profile we chose has 4 digits, unlike the wing profile.

We considered the same criteria we used in the selection of the wing airfoil in the selection of the fuselage airfoil (Mach number, Reynold number, etc.). As a result of our research, we decided to use the NACA 2414 profile as the airfoil.

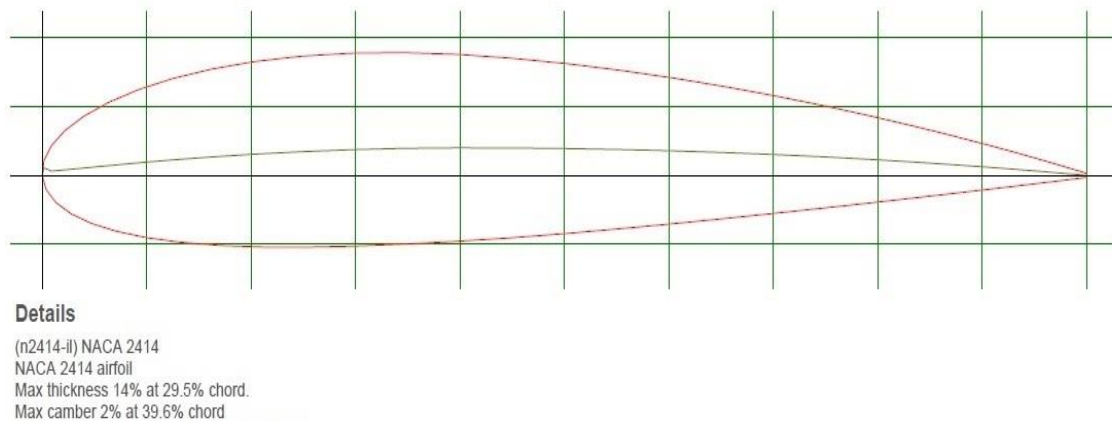


Figure 3.23. NACA 2414 (Melin, 2013)

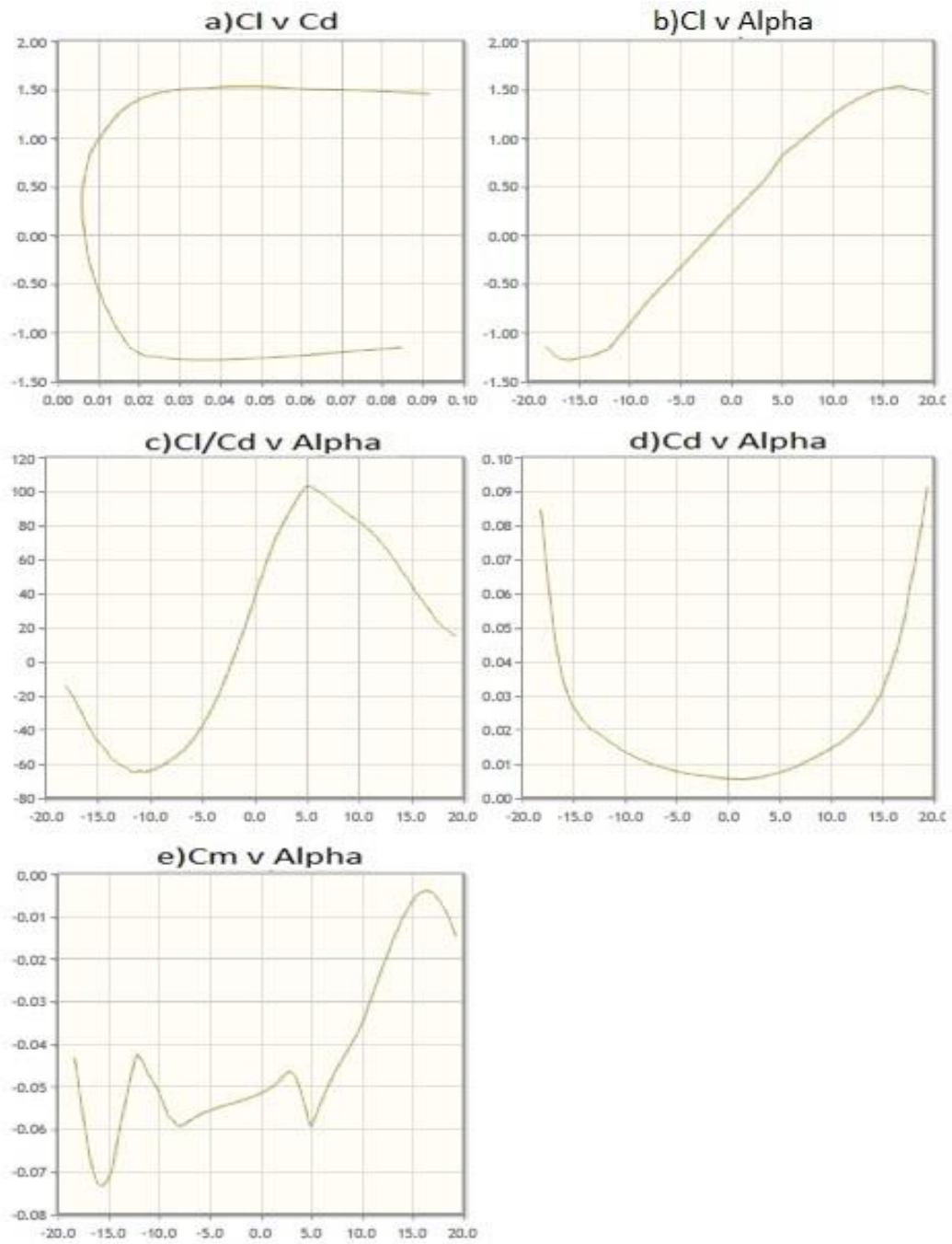


Figure 3.24. Aerodynamic coefficient graphs. a) The variations the lift coefficient versus of the drag coefficient. b) The variations of lift coefficient versus the angle of attack. c) The variations of the lift-to-drag ratio versus the angle of attack. d) The variations of drag coefficient versus the angle of attack. e) The Variations of Pitching Moment Coefficient versus Angle of Attack. (Melin, 2013)

Table 3.5. Table of coefficients for NACA 2414 depending on the changing angle of attack
(Melin, 2013)

Alpha	Cl	Cd	Cdp	Cm	Alpha	Cl	Cd	Cdp	Cm
-18.250	-1.1298	0.08491	0.08162	-0.0429	-6.000	-0.4114	0.00908	0.00348	-0.0563
-18.000	-1.1553	0.07749	0.07409	-0.0469	-5.750	-0.3843	0.00890	0.00329	-0.0560
-17.750	-1.1815	0.07006	0.06653	-0.0510	-5.500	-0.3574	0.00869	0.00311	-0.0558
-17.500	-1.2057	0.06285	0.05919	-0.0551	-5.250	-0.3303	0.00850	0.00293	-0.0555
-17.250	-1.2260	0.05617	0.05238	-0.0590	-5.000	-0.3031	0.00832	0.00278	-0.0553
-17.000	-1.2413	0.05018	0.04627	-0.0627	-4.750	-0.2758	0.00817	0.00262	-0.0550
-16.750	-1.2517	0.04505	0.04101	-0.0660	-4.500	-0.2483	0.00801	0.00248	-0.0548
-16.500	-1.2577	0.04071	0.03656	-0.0687	-4.250	-0.2210	0.00785	0.00235	-0.0546
-16.250	-1.2599	0.03715	0.03289	-0.0707	-4.000	-0.1937	0.00770	0.00223	-0.0544
-16.000	-1.2595	0.03419	0.02983	-0.0721	-3.750	-0.1661	0.00756	0.00212	-0.0543
-15.750	-1.2572	0.03174	0.02728	-0.0728	-3.500	-0.1387	0.00744	0.00201	-0.0541
-15.500	-1.2531	0.02972	0.02516	-0.0729	-3.250	-0.1112	0.00733	0.00192	-0.0539
-15.250	-1.2475	0.02806	0.02341	-0.0724	-3.000	-0.0837	0.00721	0.00183	-0.0537
-15.000	-1.2401	0.02672	0.02199	-0.0715	-2.750	-0.0562	0.00711	0.00175	-0.0536
-14.750	-1.2315	0.02560	0.02079	-0.0702	-2.500	-0.0288	0.00702	0.00168	-0.0534
-14.500	-1.2211	0.02473	0.01984	-0.0687	-2.250	-0.0015	0.00694	0.00162	-0.0532
-14.250	-1.2229	0.02346	0.01850	-0.0654	-1.750	0.0536	0.00677	0.00152	-0.0528
-14.000	-1.2227	0.02251	0.01749	-0.0617	-1.500	0.0810	0.00670	0.00148	-0.0527
-13.750	-1.2157	0.02176	0.01670	-0.0588	-1.250	0.1081	0.00661	0.00145	-0.0525
-13.500	-1.2065	0.02114	0.01604	-0.0561	-1.000	0.1351	0.00652	0.00143	-0.0522
-13.250	-1.1965	0.02060	0.01546	-0.0533	-0.750	0.1620	0.00644	0.00142	-0.0520
-13.000	-1.1862	0.02009	0.01490	-0.0505	-0.500	0.1889	0.00637	0.00142	-0.0517
-12.750	-1.1752	0.01961	0.01438	-0.0478	-0.250	0.2161	0.00631	0.00142	-0.0515
-12.500	-1.1634	0.01916	0.01387	-0.0452	0.000	0.2432	0.00625	0.00144	-0.0512
-12.250	-1.1503	0.01876	0.01342	-0.0427	0.250	0.2702	0.00622	0.00147	-0.0510
-12.000	-1.1298	0.01801	0.01262	-0.0420	0.500	0.2972	0.00620	0.00150	-0.0507
-11.750	-1.1006	0.01731	0.01189	-0.0430	0.750	0.3240	0.00619	0.00154	-0.0503
-11.500	-1.0696	0.01680	0.01136	-0.0441	1.000	0.3507	0.00618	0.00158	-0.0500
-11.250	-1.0377	0.01637	0.01089	-0.0453	1.250	0.3775	0.00616	0.00164	-0.0496
-11.000	-1.0047	0.01601	0.01048	-0.0467	1.500	0.4040	0.00617	0.00171	-0.0491
-10.750	-0.9748	0.01528	0.00974	-0.0477	1.750	0.4303	0.00620	0.00178	-0.0486
-10.500	-0.9448	0.01484	0.00929	-0.0485	2.000	0.4563	0.00624	0.00186	-0.0480
-10.250	-0.9130	0.01447	0.00888	-0.0495	2.250	0.4823	0.00630	0.00195	-0.0473
-10.000	-0.8807	0.01403	0.00841	-0.0507	2.500	0.5081	0.00639	0.00204	-0.0467
-9.750	-0.8481	0.01354	0.00792	-0.0521	2.750	0.5347	0.00650	0.00214	-0.0462
-9.500	-0.8139	0.01319	0.00756	-0.0536	3.000	0.5634	0.00661	0.00223	-0.0461
-9.250	-0.7794	0.01282	0.00716	-0.0552	3.250	0.5934	0.00675	0.00232	-0.0465

Table 3.5. Table of coefficients for NACA 2414 depending on the changing angle of attack
(Melin, 2013) (more)

Alpha	Cl	Cd	Cdp	Cm	Alpha	Cl	Cd	Cdp	Cm
-9.000	-0.7448	0.01239	0.00675	-0.0568	3.500	0.6256	0.00692	0.00243	-0.0473
-8.750	-0.7166	0.01211	0.00645	-0.0569	4.000	0.6973	0.00727	0.00266	-0.0508
-8.500	-0.6857	0.01172	0.00606	-0.0577	4.250	0.7327	0.00747	0.00278	-0.0525
-8.250	-0.6538	0.01138	0.00573	-0.0586	4.500	0.7713	0.00769	0.00291	-0.0549
-8.000	-0.6238	0.01110	0.00543	-0.0590	4.750	0.8116	0.00792	0.00306	-0.0577
-7.750	-0.5983	0.01077	0.00513	-0.0586	5.000	0.8451	0.00815	0.00321	-0.0590
-7.500	-0.5699	0.01055	0.00488	-0.0586	5.250	0.8660	0.00836	0.00334	-0.0577
-7.250	-0.5442	0.01023	0.00459	-0.0581	5.500	0.8866	0.00860	0.00349	-0.0563
-7.000	-0.5176	0.01003	0.00437	-0.0577	5.750	0.9070	0.00887	0.00367	-0.0548

3.4.2. Fuselage 3D Model Design

3D design of the fuselage; After determining the fuselage airfoil, dimensions and angle of attack, it was made in line with these data. We will use SolidWorks as the design program.

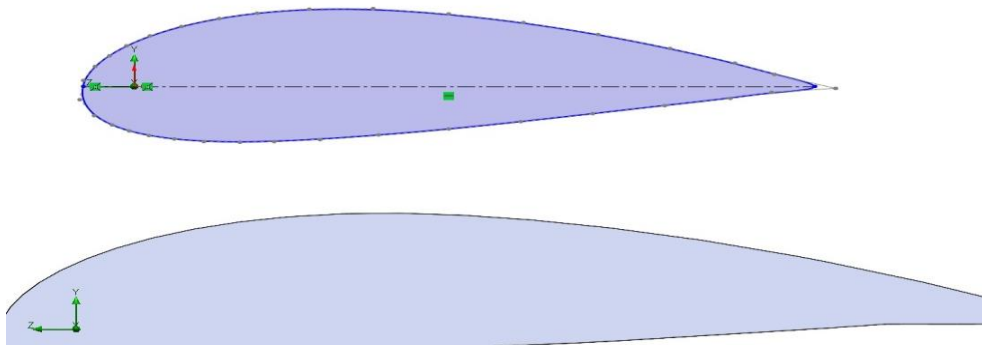


Figure 3.25. 2D Model Fuselage Airfoil



Figure 3.26. 3D Model Fuselage

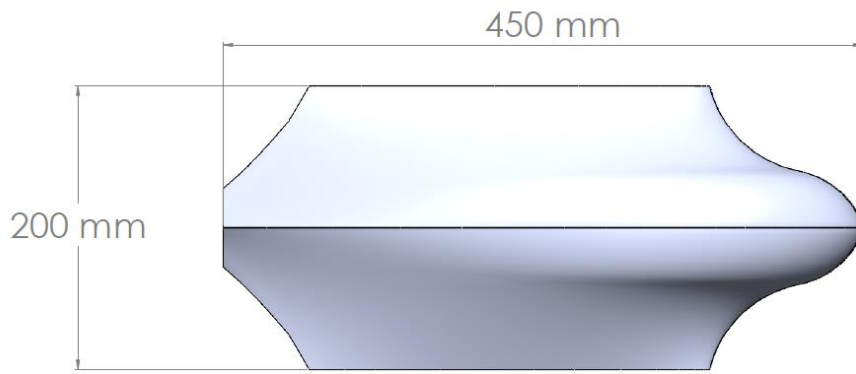


Figure 3.27. Fuselage Dimensions

3.5. Body Assembly

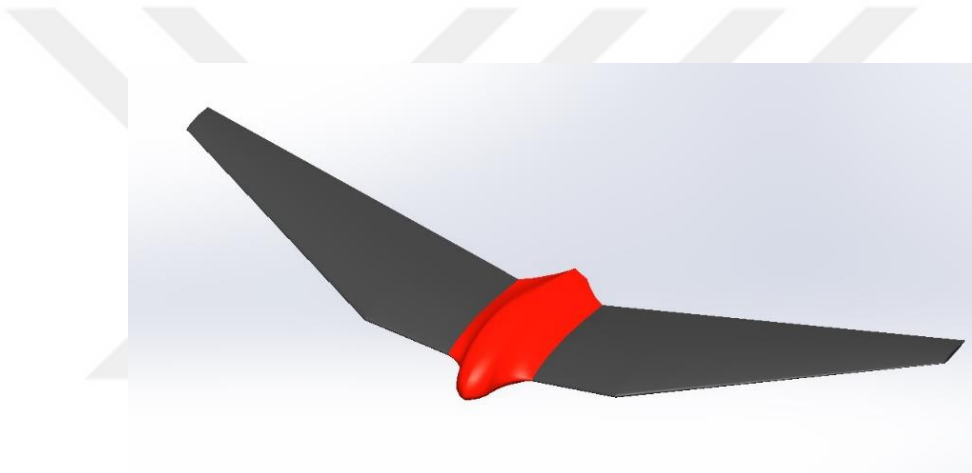


Figure 3.28. Body Assembly

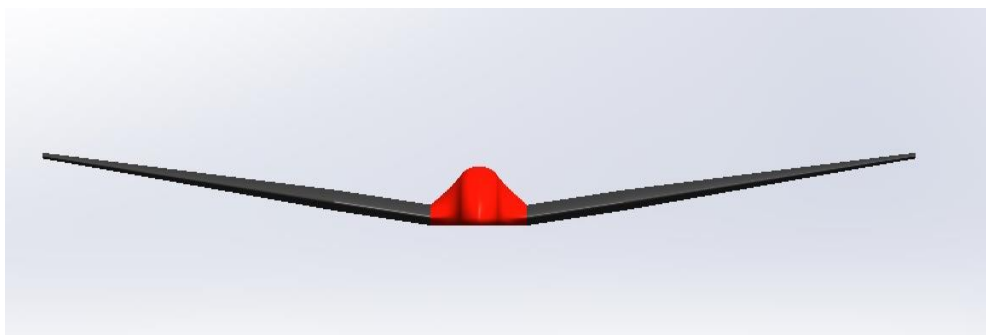


Figure 3.29. Body Assembly (Front)

4. RESULTS

4.1. Wing Flow Simulation

After completing the 3D design of the wing, flow analysis was performed using the SolidWorks Flow Simulation analysis program. In the analyzes, the distribution of flow velocity on the surfaces, dynamic pressure distribution and turbulence length were examined.

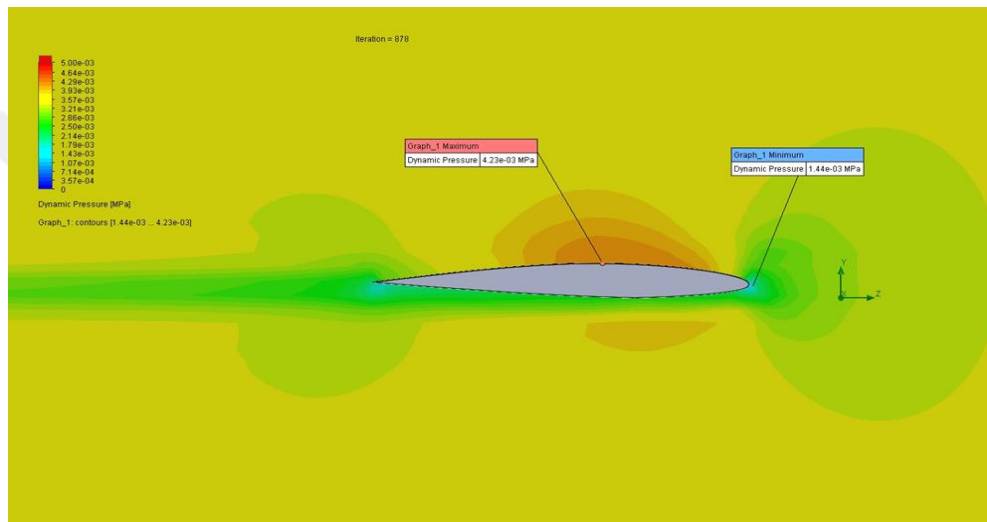


Figure 4.1. Wing Dynamic Pressure

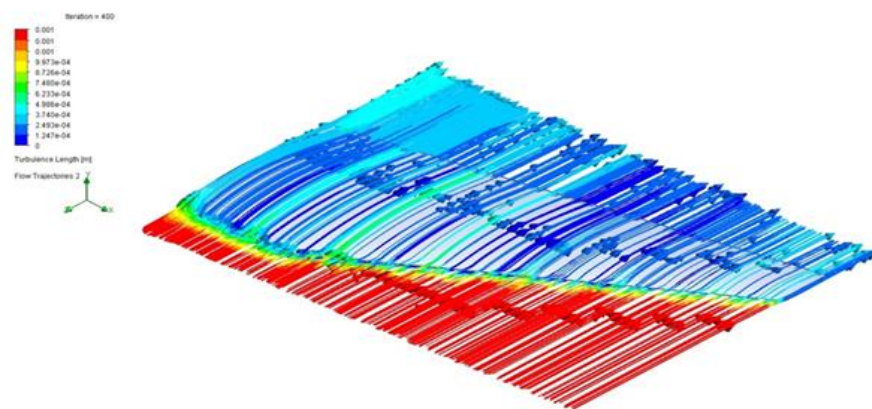


Figure 4.2. Wing Turbulence Length (Perspective)

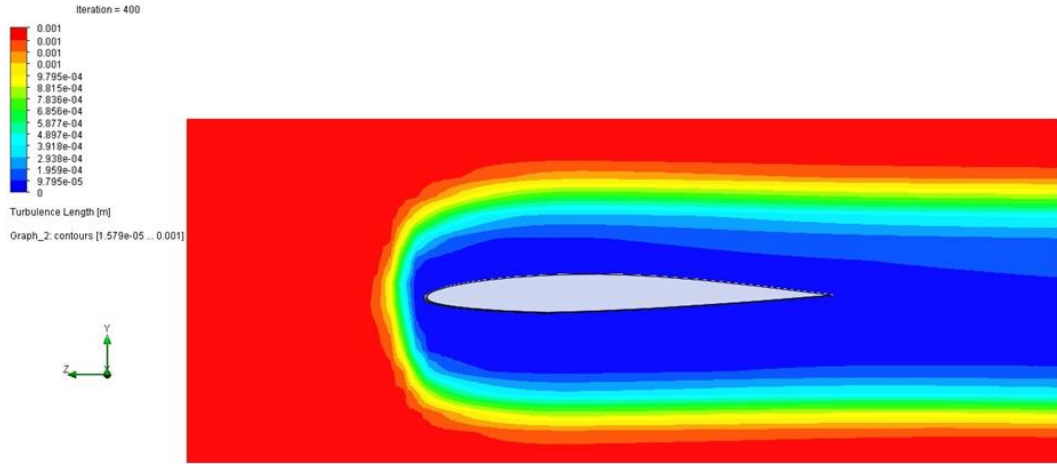


Figure 4.3. Wing Turbulence Length

Table 4.1. Wing Results

Wing						
Goal Name	Unit	Value	Averaged Value	Minimum Value	Maximum Value	Delta
Min. Total Pressure	(MPa)	0,09926084	0,099174794	0,09879725	0,09941286	5,35935E-05
Avg. Total Pressure	(MPa)	0,10492906	0,104928941	0,10492831	0,104929449	2,82598E-08
Max. Total Pressure	(MPa)	0,11347973	0,113408925	0,11329259	0,113630607	0,000110405
Max. Dynamic Pressure	(MPa)	0,00599891	0,006206091	0,00599079	0,006348285	7,01825E-05
Total Avg. Dynamic Pressure	(MPa)	0,00341691	0,003416952	0,00341646	0,003417337	2,08669E-08
Min. Velocity	(m/s)	-93,511659	-95,53759169	-97,062979	-93,47243275	0,73080821
Avg. Velocity	(m/s)	-74,59976	-74,60024627	-74,605364	-74,59371403	0,000310734
Avg. Turbulance Length	(m)	0,00122458	0,001231169	0,00122359	0,001257175	2,02766E-06
Avg. Turbulence Intensity	(%)	0,10720809	0,106967289	0,10673695	0,107266745	0,000165232
Avg. Turbulent Dispersion	(W/kg)	1,14579471	1,121844133	0,89468056	1,453582184	0,065633862
Force	(N)	19,1669206	19,14978833	17,6268166	20,83667588	0,167999752
Force (Y)	(N)	16,8227198	16,77506384	15,0347879	18,62209628	0,17722717
Force (Z)	(N)	-8,6358905	-8,68732169	-8,8937288	-8,549414491	0,039113349
Friction Force (Z)	(N)	-2,1812046	-2,198102704	-2,3779063	-2,168183548	0,01072095
Torque (X)	(N*m)	6,05160164	6,045449443	5,42368507	6,691938489	0,067223323
Avg. Dynamic Pressure	(MPa)	0,00341697	0,00341701	0,00341651	0,003417397	2,10217E-08

4.2. Fuselage Flow Simulation

After completing the 3D design of the fuselage, flow analysis was performed using the SolidWorks Flow Simulation analysis program. In the analyzes, the distribution of flow velocity on the surfaces, dynamic pressure distribution and turbulence length were examined.

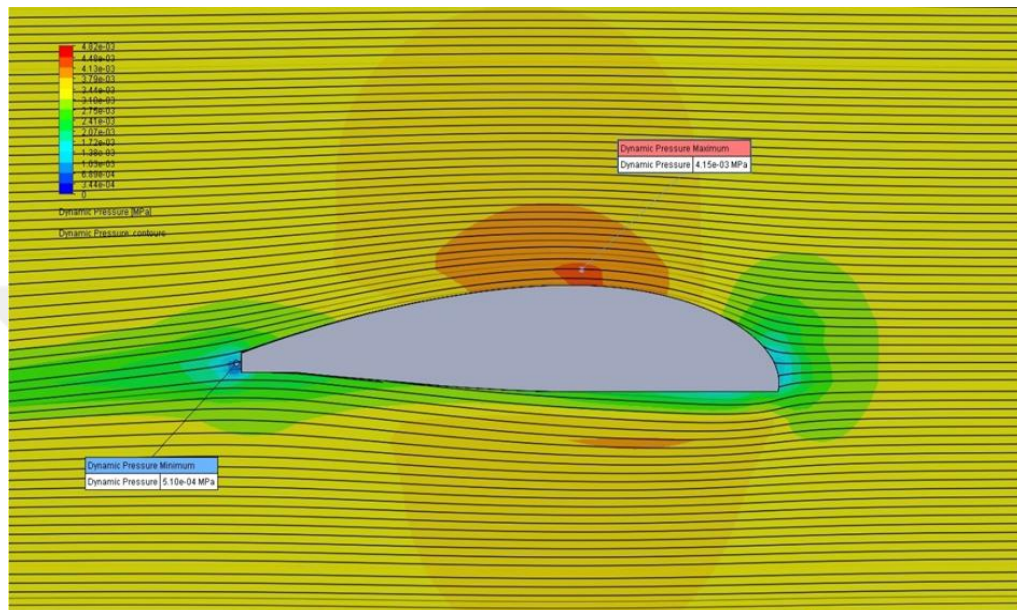


Figure 4.4. Fuselage Dynamic Pressure

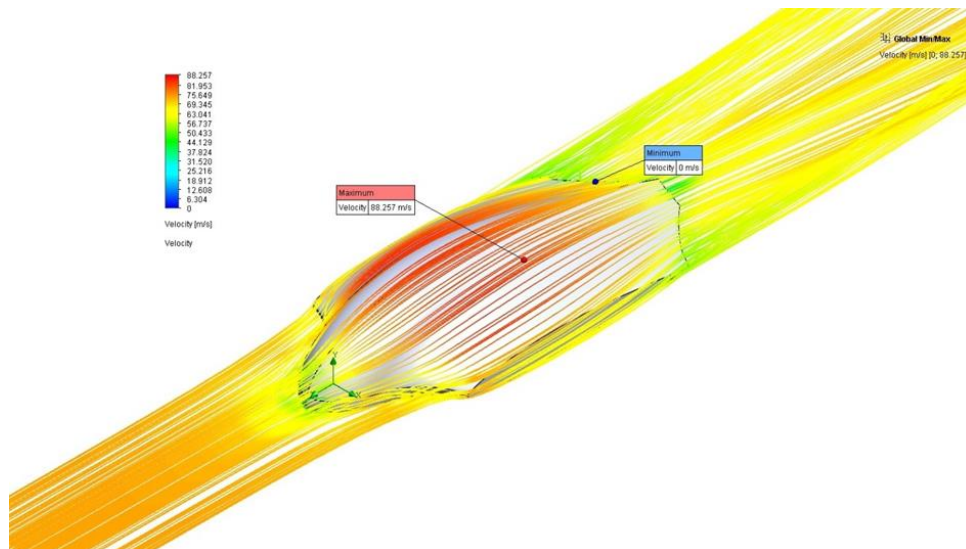


Figure 4.5. Fuselage Velocity

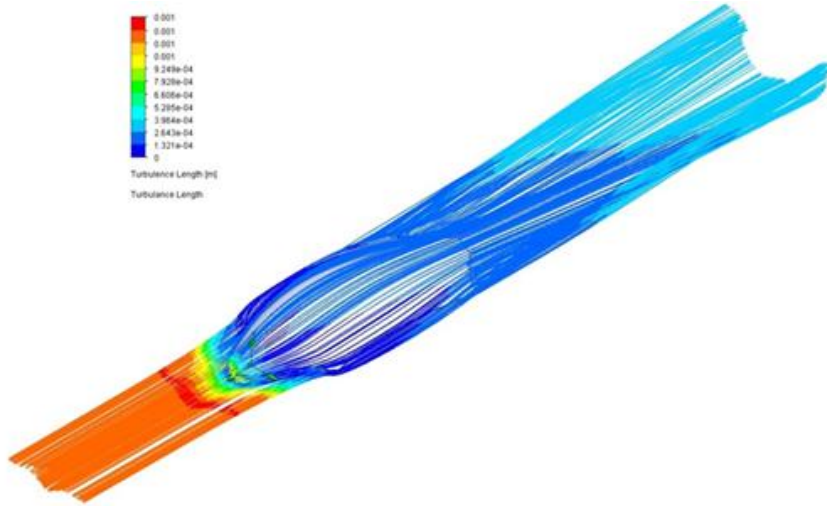


Figure 4.6. Fuselage Turbulence Length (Perspective)

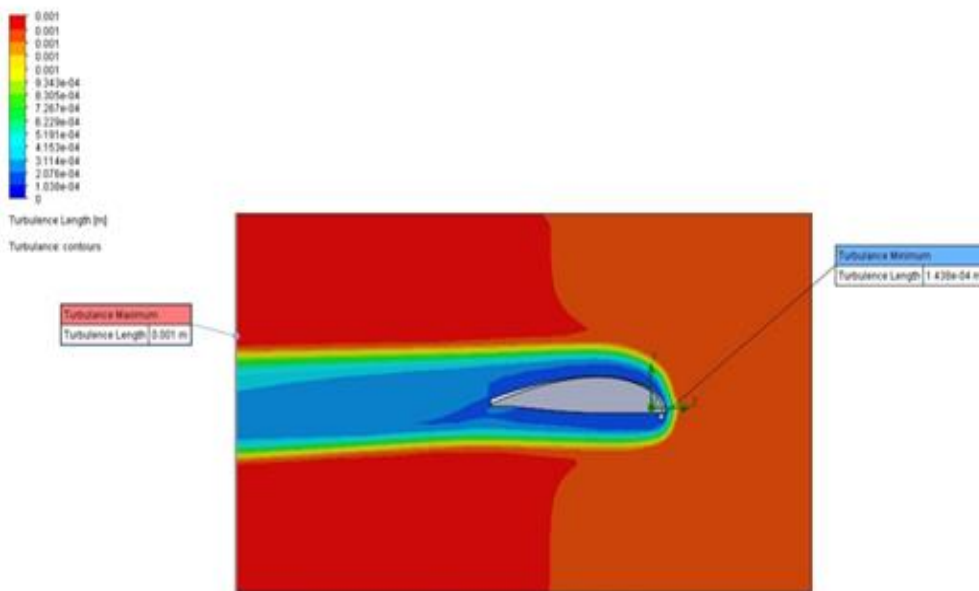


Figure 4.7. Fuselage Turbulence Length

Table 4.2. Fuselage Results

Fuselage						
Goal Name	Unit	Value	Averaged Value	Minimum Value	Maximum Value	Delta
Min. Total Pressure	(MPa)	0,09820986	0,098237403	0,09820288	0,098265168	4,7911E-05
Avg. Total Pressure	(MPa)	0,10488787	0,104887884	0,10488786	0,104887907	3,06422E-08
Max. Total Pressure	(MPa)	0,11100628	0,110961335	0,11082769	0,111106158	4,98318E-05
Max. Dynamic Pressure	(MPa)	0,00536351	0,005476236	0,00534633	0,005655766	3,46022E-05
Total Avg. Dynamic Pressure	(MPa)	0,0033657	0,003365708	0,00336569	0,003365728	3,1703E-08
Min. Velocity	(m/s)	-89,209097	-89,18469036	-89,240067	-89,10291196	0,137155325
Avg. Velocity	(m/s)	-74,055304	-74,05549851	-74,055766	-74,05523761	0,000324003
Avg. Turbulance Length	(m)	0,00131254	0,00131255	0,00131241	0,001312641	2,29741E-07
Avg. Turbulence Intensity	(%)	0,09904463	0,099036631	0,09901706	0,09906662	4,95572E-05
Avg. Turbulent Dispersion	(W/kg)	0,25147625	0,252523811	0,25107874	0,254239689	0,003160948
Force	(N)	16,3748229	16,39849487	16,2334803	16,63095013	0,097461159
Force (Y)	(N)	15,0959156	15,11760789	14,9344886	15,38158601	0,111289987
Force (Z)	(N)	-6,3440659	-6,352873169	-6,4226574	-6,302035423	0,015529813
Friction Force (Z)	(N)	-1,133429	-1,131466234	-1,1516556	-1,120877363	0,015133811
Torque (X)	(N*m)	5,63227085	5,630218956	5,59902882	5,669849042	0,031010661
Avg. Dynamic Pressure	(MPa)	0,0033657	0,003365716	0,0033657	0,003365736	3,17954E-08

4.3. Body Flow Simulation

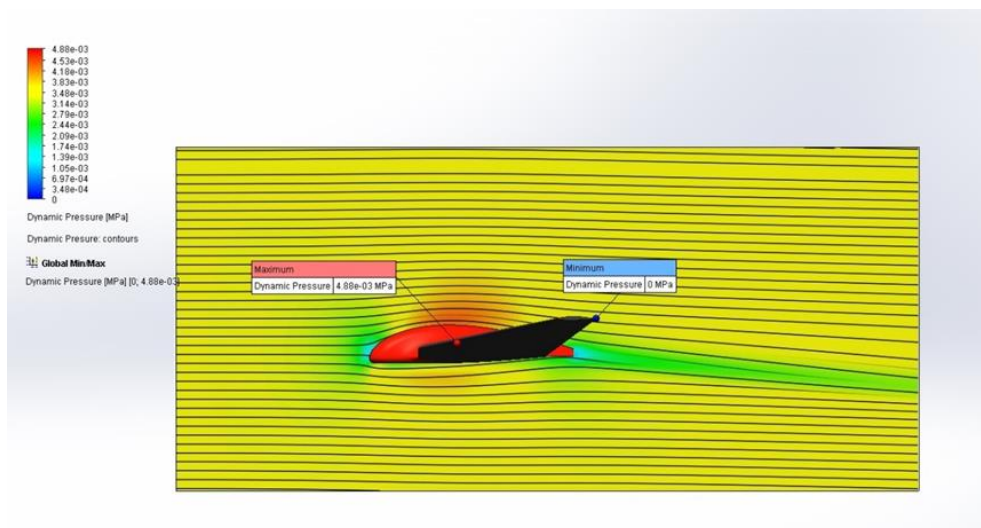


Figure 4.8. Body Dynamic Pressure

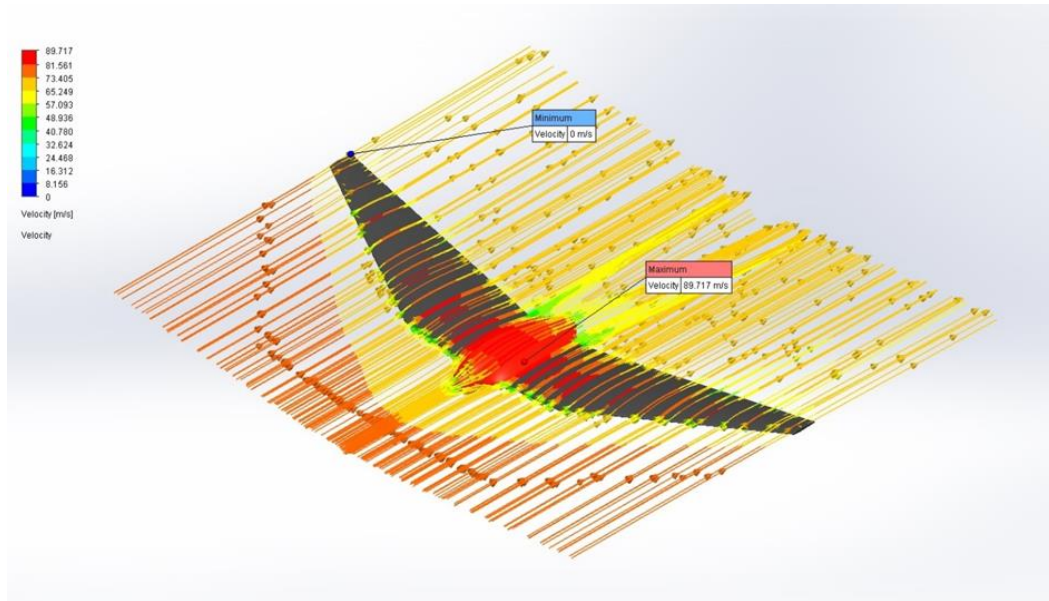


Figure 4.9. Body Velocity

Table 4.3. Body Results

Body						
Goal Name	Unit	Value	Averaged Value	Minimum Value	Maximum Value	Delta
Min. Total Pressure	(MPa)	0,09898264	0,098982742	0,0989638	0,098998113	2,31362E-06
Avg. Total Pressure	(MPa)	0,10487949	0,104879498	0,10487934	0,104879615	4,60356E-08
Max. Total Pressure	(MPa)	0,10865215	0,108687126	0,1085973	0,109235902	2,13101E-05
Max. Dynamic Pressure	(MPa)	0,00487663	0,004867764	0,00485084	0,004881011	4,38465E-06
Total Avg. Dynamic Pressure	(MPa)	0,00336027	0,003360294	0,00336011	0,003360446	5,92698E-08
Min. Velocity	(m/s)	-89,547725	-89,47177566	-89,577436	-89,35756459	0,038228395
Avg. Velocity	(m/s)	-73,990107	-73,99037391	-73,99227	-73,98794027	0,000715417
Avg. Turbulance Length	(m)	0,00127526	0,00127692	0,00126515	0,001306366	2,13518E-06
Avg. Turbulence Intensity	(%)	0,10253934	0,102566998	0,10244415	0,102656565	5,13134E-05
Avg. Turbulent Dispersion	(W/kg)	0,46011225	0,466010312	0,4438887	0,479210004	0,006935509
Force	(N)	101,1116	101,8979492	99,2991244	104,0525267	1,078414015
Force (Y)	(N)	98,1046414	98,90744437	96,2581676	101,0765467	1,105083431
Force (Z)	(N)	-24,46542	-24,49491719	-24,904723	-23,97361425	0,042099222
Friction Force (Z)	(N)	-5,9631088	-5,975237683	-6,3171651	-5,604968911	0,037881156
Torque (X)	(N*m)	29,230841	29,45670429	28,6634068	30,12366676	0,349301702
Avg. Dynamic Pressure	(MPa)	0,0033603	0,003360325	0,00336014	0,003360479	5,95418E-08

5. DISCUSSION

We saw that the NACA profiles we chose were very close to the standard values in the flow analyzes we made during the increasing design process. When we analyzed the force in the Y direction (lifting force) formed when we analyzed the entire body, we obtained a maximum value of 101 N. These values are not included in the thrust forces that will occur from the engines we will use. The useful load weight of the UAV we estimate is 15 kg (150 N). When we add the number of engines we have chosen and the thrust force above the values obtained in free flight, the total lifting force will be $7 \text{ kg} \times 3 = 21 \text{ kg}$ (210 N) total lifting force = $101 + 210 = 211 \text{ N}$ force is obtained. Since this value is higher than the payload value, the UAV can fly comfortably.

Another value we obtained from the results of the analysis is that when the dynamic pressure distribution of the UAV is examined, the maximum pressure value that occurs is 0.00487663 Mpa. This is an indication that our NACA profiles we have chosen are the right choice.

The torque value (rotational moment) occurring in the Z axis during flight is $30 \text{ N}\cdot\text{m}$. This value can be balanced with the balancing moment by adjusting the engine revolutions of the flight control card in the UAV with the UAV wing controllers. Also, this value can be balanced with the revisions to be made in the design. It can be lowered.

As a result, as a result of the flow analysis, it was understood that our UAV was suitable for flight.

6. CONCLUSION AND RECOMMENDATIONS

Whether an aircraft is a UAV or a normal one, it contains many physics rules. That's why it includes a serious calculation. It is also a sector that requires the collaboration of different engineering branches.

The concept design and analysis of the UAV, which can take off and land vertically, has been made by examining the wing and body.

Complex surface designs were avoided by considering the manufacturability at the design stage.

Before starting the designs, many UAV models were examined. By analyzing the strengths and weaknesses of the examined models, the weaknesses were tried to be improved in our own design, and the final design was obtained, and the concept design emerged.

7. APPENDICES

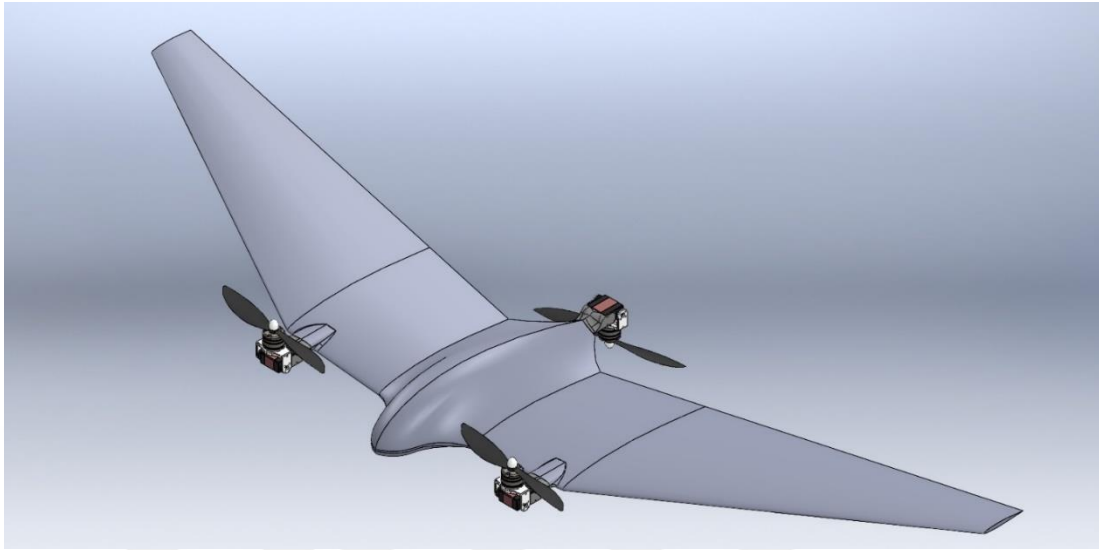


Figure.7.1.UAV Vertical Take Off Mode

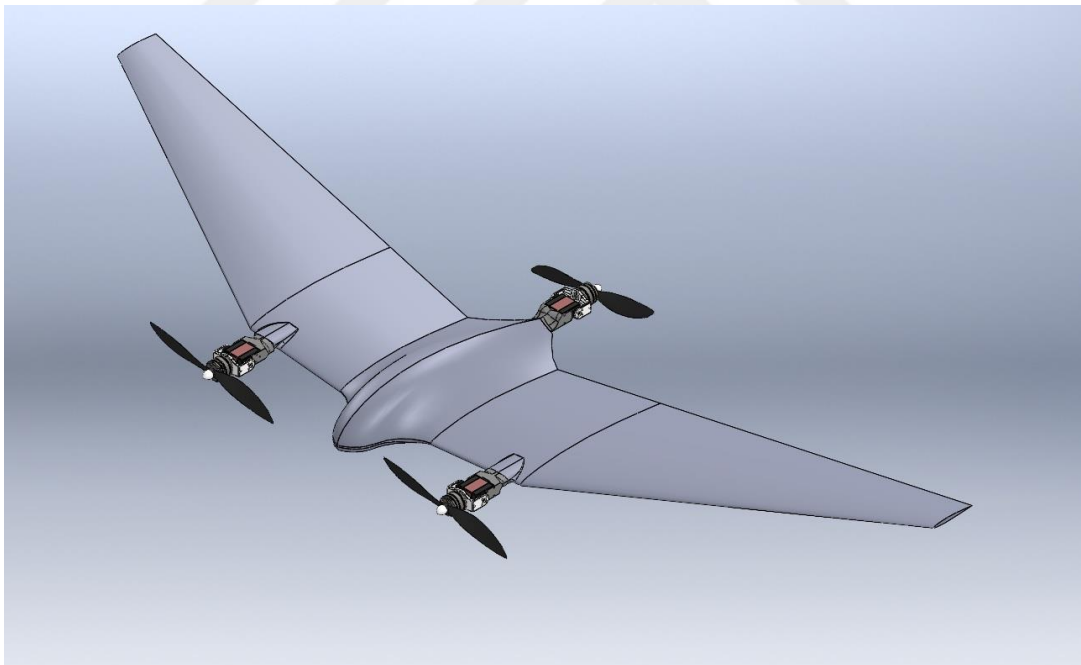


Figure 7.2. UAV Flight Mode

REFERENCES

- A. C. Kermode, Revised by R.H. Barnard & D.R. Philpott (2006). Mechanics of Flight. Pearson Education Limited Edinburgh Gate Harlow Essex CM20 2JE England. ISBN-13: 978-1-4058-2359-3.
- A. Eken (2018). Sabit Kanatlı İHA Aerodinamik ve Uçuş Mekaniği. TÜBİTAK.
- Anonymous, (2022 a). <https://www.thisdayinaviation.com/27-august-1939/> [Accessed on June, 21, 2022]
- Anonymous,(2022 b). https://en.wikipedia.org/wiki/Unmanned_aerial_vehicle#cite_note-3 [Accessed on June,16, 2022]
- Anonymous, (2022 c). https://en.wikipedia.org/wiki/Unmanned_aerial_vehicle [Accessed on June, 25, 2022]
- Anonymous, (2022 d). <https://www.lavionnaire.fr/SiteImgResAng/AeroArowProfilAng.png> [Accessed on June,20,2022]
- Anonymous, (2022 e). <https://clqtg10snjb14i85u49wifbv-wpengine.netdna-ssl.com/wp-content/uploads/2021/03/forces-on-airplane.jpg> [Accessed on May,15, 2022]
- Anonymous,(2022 f).
https://en.wikipedia.org/wiki/Reynolds_number#:~:text=The%20Reynolds%20number%20is%20the,the%20interior%20of%20a%20pipe. [Accessed on May,22, 2022]
- Anonymous,(2022 g).
<https://www.webtekno.com/images/editor/default/0003/48/bccae51e2603f70014ea16c2619c7f870fefc9d0.jpeg> [Accessed on June, 10, 2022]
- Anonymous,(2022 h).
<https://catimes.brightspotcdn.com/dims4/default/5780eb8/2147483647/strip/true/crop/2498x1096+0+0/resize/2000x878!/quality/90/?url=https%3A%2F%2Fcalifornia-times-brightspot.s3.amazonaws.com%2F83%2F8fa954334567861ef0fa39669d54%2Fsd-graphics-793870-w1-sd-g-predator-drone.jpg> [Accessed on May, 10, 2022]

- Britannica, The Editors of Encyclopaedia. "aerodynamics". Encyclopedia Britannica, 12 Aug. 2019, <https://www.britannica.com/science/aerodynamics>. [Accessed on June,6, 2022]
- D. Raymer (2018). Aircraft Design: A Conceptual Approach, Sixth Edition, Published by the AIAA Education Series American Institute of Aeronautics and Astronautics, Inc. 1801 Alexander Bell Drive, Reston, Virginia 20191-4344, ISBN 978-1-60086-911-2
- Hüseyin Şahin, Tuğrul Oktay (2019). Properties of Novel Tricopter And Comparison of Other Unmanned Aerial Vehicles,816-825, DOI:10.31590/ejosat.586900.
- Mohammad H. Sadraey (2013). Aircraft Design A Systems Engineering Approach. John Wiley & Sons Ltd, The Atrium, Southern Gate, Chichester, West Sussex, PO19 8SQ, United Kingdom.
- Tomas Melin (2013). Parametric Airfoil Catalog, Part II,An Aerodynamic and Geometric Comparison Between Parametrized and Point Cloud Airfoils. Linköping University LiU-Tryck 581 83 Linköping SWEDEN. ISBN: 978-91-7519-656-5
- U.S. Department of Transportation Federal Aviation Administration Flight Standards Service (2016). Pilot's Handbook of Aeronautical Knowledge. United States Department of Transportation, Federal Aviation Administration, Airman Testing Standards Branch, AFS-630, P.O. Box 25082, Oklahoma City, OK 73125.
- U.S. Department of Transportation Federal Aviation Administration (2016).Pilot's Handbook of Aeronautical Knowledge, United States Department of Transportation, Federal Aviation Administration, Airman, Testing Standards Branch.
- Y. Volkan Pehlivanoğlu (2013). Havacilik ve Uzay Çalışmalarinin Tarihsel Gelişimi. Hava Harp Okulu Matbaasi, İstanbul .

T.C.

AYDIN ADNAN MENDERES UNIVERSITY

GRADUATE SCHOOL OF NATURAL AND APPLIED SCIENCES

SCIENTIFIC ETHICAL STATEMENT

I hereby declare that I composed all the information in my master's thesis entitled EAGLE EYE within the framework of ethical behavior and academic rules, and that due references were provided and for all kinds of statements and information that do not belong to me in this study in accordance with the guide for writing the thesis. I declare that I accept all kinds of legal consequences when the opposite of what I have stated is revealed.

Kadir KARACA

29/07/2022

CURRICULUM VITAE

Last name, First name : KARACA, Kadir

WORK EXPERIENCE

Year Place/Institution Title

:

- 2011-2017 Alpler Ziraat Aletleri A.Ş. / Agricultural Machinery And Equipment Designer
- 2017-2021 Alpler Ziraat Aletleri A.Ş. / Manager of R&D Department
- 2022- Present Mahindra & Mahindra ltd/ COE Office Manager

ACADEMIC PUBLISHING

1. ARTICLES

- Material Characterization Of Rotary Slasher Cutter Blades

Authors: Prof.Dr. Ismail BOGREKÇİ ,Prof.Dr.Pinar DEMIRCIOGLU,
Kadir KARACA.